FACULTY OF SCIENCE, ENGINEERING AND AGRICULTURE
DEPARTMENT OF EARTH SCIENCES

Influence of firing temperature on ceramic properties of kaolinitic clays from Duthuni, Limpopo Province (South Africa)

by

Mihleketo Oscar Miyambu
(11501405)

A Dissertation Submitted to the Department of Earth Sciences, Faculty of Science, Engineering and Agriculture in Fulfilment of the Requirements for the Master of Earth Sciences in Mining and Environmental Geology

Supervisor: Prof L. Diko-Makia

Co-supervisor: Snr Prof G.E. Ekosse

Declaration

I, **Mihleketo Oscar Miyambu**, Student Number **11501405**, declare that this dissertation, submitted to the Department of Earth Sciences, Faculty of Science, Engineering and Agriculture is my own work and has not been previously submitted in whole or in part for any degree. All assistance and information from published and unpublished work has been fully acknowledged.

19/04/2024

Miyambu MO

Date

Dedication

I would love to dedicate this research to the owners, directors and all the staff members at Duthuni Kaolin Mine (Vhavenda Bricks), who afforded me with access and resources to conduct this research project.

Acknowledgements

I want to acknowledge Prof. L Diko Makia, who has been very patience with me throughout the project. Your supervisory skills and knowledge in Applied Clay Science have made this piece of work possible. I would love to thank my co-supervisor for the technical assistance with data analysis. Thank you to Mr. Honey Xivuri. My brother; your financial investment on my education has never been wasted. I have also benefited a lot from MINTEK, who covered the Laboratory costs for this research project.

I give honour and Glory to Almighty God, who has kept me till this far.

Abstract

This study investigated the ceramic suitability of two representative kaolin samples from Duthuni area, subjected to four firing temperatures (800 ^{o}C, 900 ^{o}C, 1000 ^{o}C and 1100 ^{o}C).The objectives were to ascertain the effects of the raw clay physical, mineralogical, chemical characteristics on its ceramic potential, elucidate on the thermal evolution and associated mineral phase transformations, and to technologically characterize the raw clays. Physical properties were identified by particle size distribution, consistency limits and clay activity. Mineralogical and chemical properties were investigated by XRD, FTIR and XRF. Firing characteristics were measured by weight loss (WL), bulk density (BD), linear shrinkage (LS), water absorption (WA) and flexural strength (FS).

The characteristic mineral assemblage comprised; quartz + kaolinite ± mica + microcline + goethite + hematite + anatase + ilmenite. Quartz occurred as major constituent in both samples, while kaolinite, Goethite and Anatase are present as minor constituents. Visual appraisal of the clay workability chart indicated that D1 and D2 plot within the high shrinkage field, with D1 displaying comparatively higher potential for shrinkage than D2. The potential for high shrinkage suggests possible detrimental effects during clay body formulation (extrusion and molding) as well as firing phases of the ceramic manufacturing process.

Interpretations drawn from the Holtz and Kovacs diagram are consistent with the mineral phases identified by XRD. Kaolinite was the main clay mineral in both samples, occurring as minor constituent. The loam to silty texture of D2 and and D1 respectively are consistent with the predominance of quart phases revealed by the XRD and Si – O functional groups observed in the IR.

The studied materials are siliceous (SiO_2: 38.5–45.5 wt%), aluminous (Al_2O_3: 23.9–16.7 wt%) and ferruginous (Fe_2O_3: 23.5–21.3 wt%), with the SiO_2/A Al_2O_3 ratios ranging from 1.61 to 2.71. The geochemistry of the clay samples also shows relatively high amounts of TiO_2 (2.91 – 2.71 wt% respectively for D1 and D2). Low kaolinite content and high iron oxide contents equally suggests kaolin impurity and colouring effect on the fired clays. Furthermore, appraisal of the ceramic suitability of D1 and D2 based on their geochemistry indicates suitability for red bodies (D2) and a close outlier for red bodies and porous tiles

The DSC curve portrayed three endothermic peaks; 85 ^oC to 90 ^oC, 295 ^oC to 300 ^oC and 530 ^oC to 535 ^oC corresponding to elimination of adsorbed water, goethite dehyroxylation and formation of metakaolinite respectively. A weak exothermic was observed at 945 ^oC and 955 ^oC suggesting recrystallization of metakaolinite to spinel or mullite. Small mass loses where observed between 20 ^oC to 120 ^oC (2% - 7.2%), 250 ^oC to 320 ^oC (1.3% - 3.8%) and 400 ^oC to 600 ^oC (5.2% - 6.2%). The relatively low kaolinite dehydroxylation temperature (535 ^oC) coupled with the generally asymmetric shape of the endothermic peaks suggests a poorly ordered and crystalline structure.

The highest percentage of weight loss (WL) was recorded at 1100 ^{o}C in D1(12.41%) and at 900 ^{o}C in D2 (16.96%). The bulk density (Bd) increased with firing temperature in both samples. The LS in D1 ranged from 10.2 % to 18.59% from 800 ^{o}C to 1100 ^{o}C. A corresponding increase in LS was also observed in D2 (8.06 % to 11.8%).The FS of D1 increased steadily up to 1000 ^{o}C and then experienced a slight decline at 1100 ^{o}C. The FS values for D1 ranged from 0.86 to 1.25 MPa, with acceptable strength attained at 1000 ^{o}C and 1100 ^{o}C. The FS of D2 showed a similar increasing trend and slight decline at 1100 ^{o}C. The WA for D1 showed a decrease with firing temperature, ranging from 24.48 % at 800 ^{o}C to 9.01% at 1100 ^{o}C. A similar trend was observed for D2 (19.39 % to 10.88 %) from 800 ^{o}C to 1100 ^{o}C respectively. D2 satisfies the conditions for massive bricks, ceramic blocks and roof tiles. The studied clays show moderate potentials for exploitation based on their inherent characteristics (without modification). This, however, limits the exploitation to predominantly face bricks. Beneficiation is thus recommended to increase value and range of structural ceramic applications.

Key words: kaolinite, ceramics, technological property, sintering, thermal behaviour

Table of Contents

List of Figures

List of Tables

Acronyms and Symbols

µm	Micrometer
Å	Ångstrom
Wt%	Weight percent
XRD	X-Ray Diffractogram
XRF	X-Ray Fluorescence
FTIR	Fourier Transform Infra-red
DSC	Differential Scanning Calorimetry
TGA	Thermogravimetric Analysis
DTA	Differential Thermal Analysis
PCE	Pyrometric Cone Equivalent
MOR	Modulus of Rupture
PSD	Particle Size Distribution
WL	Weight Loss
BD	Bulk Density
WA	Water Absorption
LS	Linear Shrinkage
FS	Flexural Strength

CHAPTER ONE: INTRODUCTION

1.1 Background

1.1.1. Clay usage in ceramics

Modern society uses clays in an ever-increasing quantity, making this category of minerals, industrial minerals for the future (Ekosse, 2005, Shemang et al., 2007). Clays and clay minerals have been widely used as the main raw materials in the fabrication of diversified ceramic products for construction materials such as bricks and tiles due to many of their specific properties before and after firing (Lee and Yeh, 2008; Mohmoudi et al., 2008; Murray, 2007). Ceramic application remained the principal consumer of clayey materials throughout the world (Ekosse and Maluba, 2006; Ekosse et al., 2007).

1.1.2. Kaolins in Africa

1.1.2.1. Kaolins geneses, deposits and occurrences in Africa

The geneses of African kaolins are reported as primary, hydrothermal, residual, mixed and secondary. According to Ekosse (2010), fifty percent of the reported kaolins were of sedimentary origin, and 35% were primary kaolins. The primary kaolins were located mainly in Central and Southern Africa. The hydrothermal kaolins were found dominantly in Central and West Africa. North African kaolins were mainly of secondary clays. Very substantial deposits and occurrences in Southern and West Africa were also secondary kaolins of sedimentary origin.

Although kaolin was found to occur quite extensively in several African countries, its industrial application is considerably low (Ekosse, 2010). Most of the kaolin deposits and

occurrences are easily accessible and can be processed and beneficiated. With these in mind, any exploration of kaolin in Africa should focus on investigating Cretaceous and Tertiary argillaceous sediments. Precambrian and Permian argillaceous sediments were also found to host kaolins of mineable quantities.

1.1.2.2. Kaolins usage in Africa

The main uses of the kaolins were for the manufacturing of ceramics, tiles, bricks, pottery, medicines, and as fillers. According to Ekosse (2010), in terms of regional distribution and main uses were as follows: Central Africa = ceramics, bricks and pottery; East Africa = bricks; North Africa = ceramics and bricks; Southern Africa = ceramics bricks and fillers; and West Africa = ceramics, bricks, pottery, medicines, and refractory. These applications are standard for kaolins from other parts of the world. Other important applications of the kaolins included absorbents, paints, paper, pesticides, rubber and refractory.

In Cameroon, Central Africa, there were few traditional factories using kaolin for the manufacturing of different types of bricks. The pottery industry also utilizes some of the country's kaolin in the making of ceramic figurines and utensils. However, the kaolin minerals found in Cameroon are highly under-utilised. A vast potential exists for use of kaolins in Cameroon in the manufacturing and construction industries. The construction industry uses kaolinitic clay for the fabrication of different types of bricks. The utilization of kaolin from Cameroon in the fabrication of sanitary ware, wall tiles, electrical and industrial porcelain and terracotta is yet to be fully attained.

Investigations on usage of kaolins from Kenya, East Africa, depicted applications in several industries including ceramics, medicines, paper, paint, and rubber product (Chandrasekaran et al., 1990). Potential resources of kaolin in Kenya were very large, though they are suitable as fire-clay (Pohl and Horkel, 1980). Kaolin around Kenya Lakes Victoria region are used in the pottery industry (Aduba et al., 1999), those from Southwest Kenya are utilised as potting clays (Langdon and Robertshaw, 1985).

Bacterial and viral load in water is removed through the aid of locally produced ceramic filters made from Kenyan kaolin (Massachusetts Institute of Technology, 2004) it should also be noted that kaolinite from Pugu kaolins in Tanzania, East Africa, serves as reference clay mineral for the identification of Kaolinite – 1md (29-1488) (ICDD, 2001).

In North Africa, Egyptian kaolins have a wide range of industrial applications which include the fabrication of tiles, bricks and ceramics (El-Dine et al., 2004). Kaolins in the Tushki area of Egypt are widely used as raw materials for the manufacture of porcelain stoneware tiles (Aly, 2002). The Egyptian kaolins are equally used for the production of pottery vessels that serve a wide variety of functions, which include cooking and domestic purposes, storage of cosmetic oils, storage and transportation of food and bricks and are used in temple and funeral rituals (Hope, 2001).

Studies conducted on Botswana kaolins revealed that they were suitable in the manufacturing of bricks, ceramic ware and sanitary ware (Ekosse, 1994, 1998; Nkoma and Ekosse, 1999; Ekosse, 2000; Ekosse and Nkoma, 2000; Ekosse, 2001a, b; Ekosse and Vink, 2001; Ekosse et al., 2003).

Previous investigations (initiated by the United Nations Development Programme in 1997) in the clay occurrences and applications in Botswana were directed towards the production of bricks for construction of houses. This was a strategic move in solving the teething housing problem that had menaced the country for several years. Currently there few factories that use kaolinitic clay for the manufacture of bricks, terracotta and tiles in Botswana (Ekosse, 2010). Pottery industries at Thamaga, Francistown and Gabane produce figurines and utensils.

1.1.3. Kaolins usage in South Africa

In 2002, South Africa was ranked No 27 in the world production of kaolin. The kaolins are primarily used in the ceramics and paper industries. Also, South African kaolins are applied as functional fillers, and used in refractories (Department of Minerals and Energy, 2005).

Kaolin exploitation remains a financial sustained profit-making mining industry that continues to contribute positively to national economies of the world (Ekosse, 2010). In South Africa, kaolinitic clays from Duthuni area (Limpopo Province) are currently being exploited for structural ceramic (mainly bricks) as Vhavhenda Bricks. Vhavhenda Bricks is one of only 6 accredited brick manufacturing plants in Limpopo Province (Clay Brick Association, 2013).

1.2 Statement of the problem

However, the use of these clayey soils is accompanied by significant problems at different stages of its exploitation and product manufacturing; especially during calcination (firing). Common process-generated problems encountered includes bloating, exploding,

fracturing, peeling, shivering and warping (Diko et al., 2011). These problems tend to affect the quality and market value of the finished products. Kaolins are not effectively characterized in terms of their technological applications.

1.3 Motivation

Kaolin market has a strong economic potential in the country. It is imperatively crucial to the government and industrialists to realize the industrial potentials of kaolin mining and processing in South Africa. This knowledge will be utilized to benefit the national economy and investment opportunities. With increasing new industrial applications of the clay minerals, any promising deposit is worth investing in.

Process-generated problems encountered during calcination, can be directly related to the genesis, physiochemistry, mineralogy, geochemistry and thermal behaviour of the raw clay (Murray, 2007; Dominguez et al., 2010; Diko and Ekosse, 2013). For optimal exploitation of the kaolinitic clays from Duthuni, there is a need for in-depth appraisal of the raw material characteristics. Although these clayey materials have been geologically, mineralogically, and geochemically characterised (Diko, 2012), their thermal behaviour and technological properties have not been appraised.

1.4 Aim and objectives

1.4.1 Aim

To study the influence of firing temperature on ceramic properties of kaolinitic clays from Duthuni.

1.4.2 Objectives

- To evaluate the effects of clay physical, mineralogical, and chemical property on ceramic suitability of duthuni kaolin,
- To characterize the thermal evolution of ceramic raw materials, and
- To investigate the technological properties of the raw clay at four firing temperatures

1.5 Description of the study area

Duthuni Kaolin is about 4 km from Thohoyandou, in the Thulamela Municipality, Vhembe District of Limpopo Province, precisely at longitude 30º 23' 23" E and latitude 23º 00'16" N (Fig.1.1). The municipality has a mountainous relief with peaks up to 2000 m above sea level. Its climatic regime is quite similar to that of the province, however mean daily temperature in summer is slightly higher (> 31ºC).

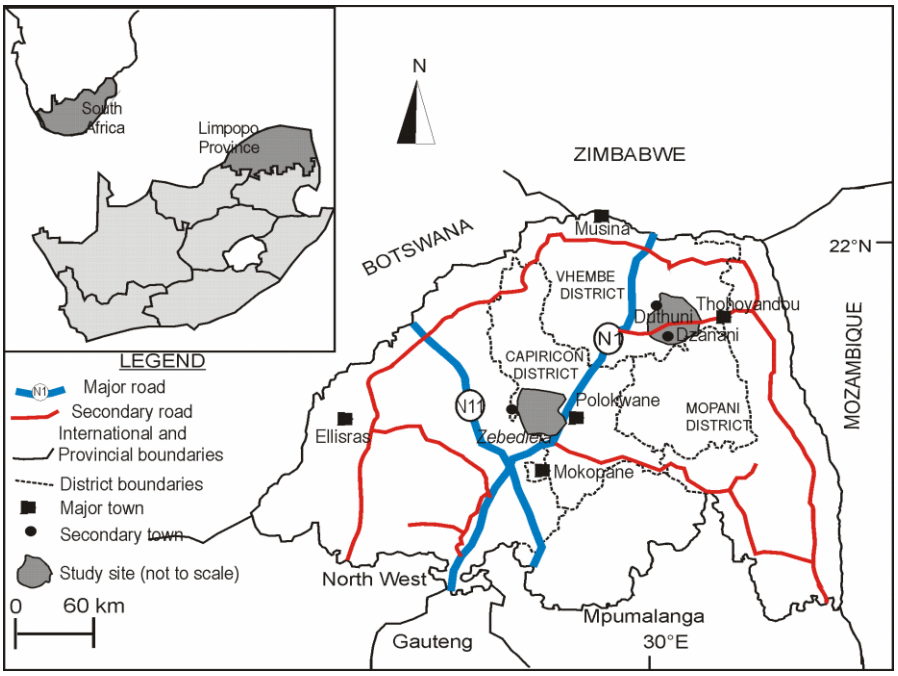

Figure 1.1 Map showing the study area.

With an area of about 2700 m2 and average thickness of 28 m, the mineable kaolin within the main excavation pit is estimated at 75, 600 m3 of which over 50 % has been mined. Kaolin is currently being mined under the trade name Vhavenda Bricks, with its main use being brick making.

1.6 Thesis overview

This study is presented in five chapters. Chapter One is the introduction which involves the background of the work, problem statement, aim and objectives of study. Chapter Two summarises the relevant literature in relation to the area of study area and factors controlling thermal characterization of structural ceramics. Chapter Three describes the experimental procedure employed in the study. The results for raw clay characterisation and technological appraisal are presented in Chapter Four. Chapter Five elaborates on the findings and draws conclusions on the ceramic suitability of the studied clays.

CHAPTER TWO: LITERATURE REVIEW

2.1 Regional geologogic setting of Duthuni Kaolin

The geology of Duthuni area is dominated by the Soutpansberg Group. The rocks of this group belong to the Proterozoic and rested unconformably on gneisses of the Limpopo Belt (Fig. 2.1). Along the eastern and most of the northern margin, the Soutpansberg outcrops were unconformably overlain by or tectonically juxtaposed against rocks of the Karoo Supergroup. The Soutpansberg Group represents a volcano-sedimentary succession subdivided into seven formations however, only four formations; Tshifhefhe, Sibasa, Fundudzi and Willie's Poort Formations occur within the vicinity of the Duthuni Kaolin occurrence (Fig. 2.1).

The basal discontinuous Tshifhefhe Formation was only a few meters thick, and made up of strongly epidotised clastic sediments, including shale, greywacke and conglomerate. The succeeding Sibasa Formation was dominantly volcanic with rare discontinuous intercalations of clastic sediments. The volcanics comprised subaerially extruded basalts and minor pyroclastic materials. The clastic sediments comprising quartzite, shale and minor conglomerate, reached a maximum thickness of 400 m. The overlying Fundudzi Formation was developed only in the north and wedges out towards the west (Fig. 2.1). It consisted mainly of arenaceous and argillaceous sediments with a few thin pyroclastic horizons. Near the top of the succession, an approximately 50 m thick layer of epidotised basaltic lava was intercalated with these sediments.

The uppermost unit was represented by the Willie's Poort Formation. A predominantly clastic succession, this formation outcropped mainly towards the northern most region of the study area. Resistant pink quartzite and sandstone with minor pebbles dominated the succession, reaching a maximum thickness of 1500 m. Conspicuously absent from the study area are the Stayt Formation regarded as a correlative of the Sibasa Formation and the Nzhelele and Mabiligwe Formations – the youngest units within the Soutpansberg Group.

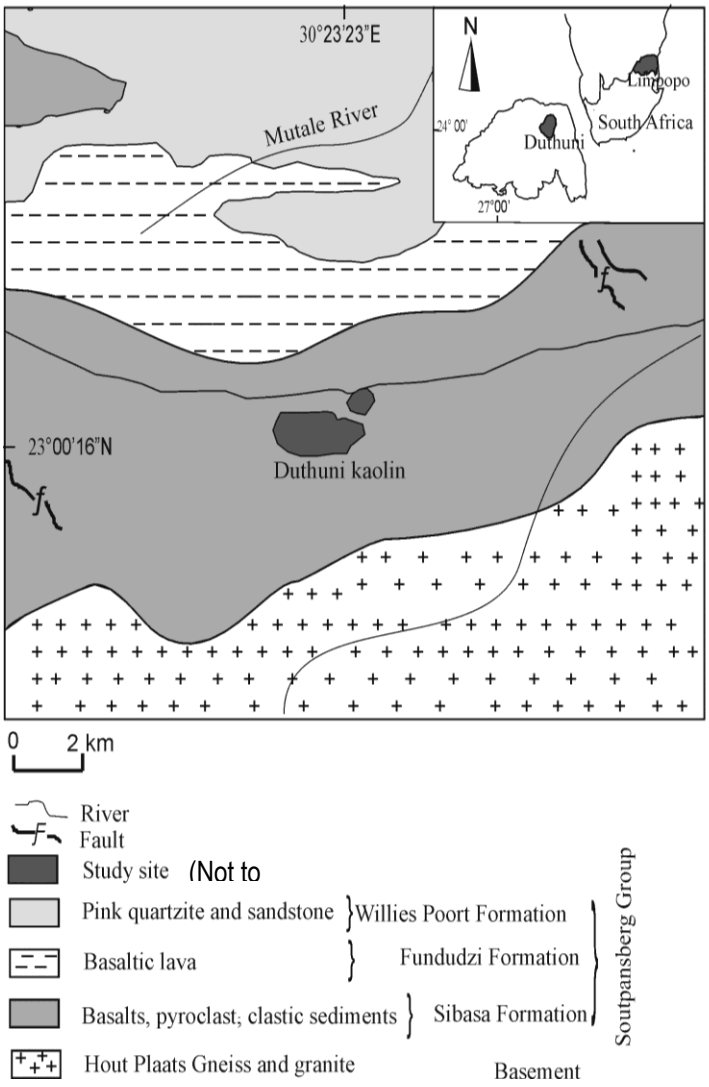

Figure 2.1 Geologic map of study area (Duthuni kaolin deposit)

2.1.1 Geology and stratigraphy of the Soutpansberg Group

The Duthuni Kaolin occurred within the Sibasa Formation – a dominantly volcanic succession (Fig 2.2). The footwall comprised basalts which were subaerially extruded. The basalts were amygdaloidal and massive. They were overlain by pyroclastic materials considered as host rocks of the kaolin. Within the main excavation pit, six distinct horizons were identified (Fig. 2.2).

	ERATHEM	GROUP	FORMATION	LITHOLOGY
PHANEROZOIC	UNDIFFERENTIATED KAROO SEQUENCE			
PROTEROZOIC	MOKOLIAN	SOUTPANSBERG	Willies Poort	Pink quartzite and sandstone with minor pebbles (Max 1500 m)
			Fundudzi	Epidotised basaltic lava intercalated with sediments (Max 50 m)
			Sibasa	Basalts, pyroclastic rocks, rare discontinuous intercalations of clastic sediments (400 m)
			Tshifhefhe	Clastic sediments, shale greywacke, conglomerate (Max 9 m)
ARCHEAN BASEMENT COMPLEX			Hout Plaats gneiss and granite	

Figure 2.2 Lithostratigraphy of Duthuni Duthuni area

The undifferentiated basaltic bed rock was overlain by a very pale pink to cream clay unit (14 m thick), followed by a yellowish-brown stratum. The thickness of the latter varied across the pit from 1 m at the edges to about 3 m towards the centre. This horizon was equally characterised by the presence of partially weathered pyroclastics (probably tuff).

Towards the centre of the pit a dark brown layer, limited in extent (1.5 × 3 m) was intercalated between the bed rock basalts and overlying yellowish brown stratum. A 2 to 8 m thick, pale red to pink stratum followed this succession immediately. Overlying this horizon was a 3 m thick, dark red, iron-rich unit with a grain-supported matrix. The boulders and pebbles did not display any preferred orientation thus were of little assistance in ascertaining the genetic history of the kaolin. A relatively thin topsoil (maximum thickness 1 m) capped the kaolin outcrop. The argillaceous sediments were about 20 m thick with two representative kaolin profiles of about 13 to 16 m identified (Fig. 2.3).

Figure 2.3 Partial view of Duthuni Kaolin quarry showing main horizons and structural controls.

Structurally, the Soutpansberg strata were tilted towards the north and truncated by many extensional faults. Within the study area two fault systems were recognized, trending towards the NW and WNW (Fig. 2.3) antithetic to the regional ENE strike of the Group. The rocks within the study area were unfoliated but in places, slightly fractured. Within the main excavation pit (Fig. 2.3) the strata dipped towards the center of the pit at an angle of 10º – 30º, adjoining the footwall basalts. The thickest kaolin unit (14 m) was observed outside the V-shaped trough (Fig. 2.4).

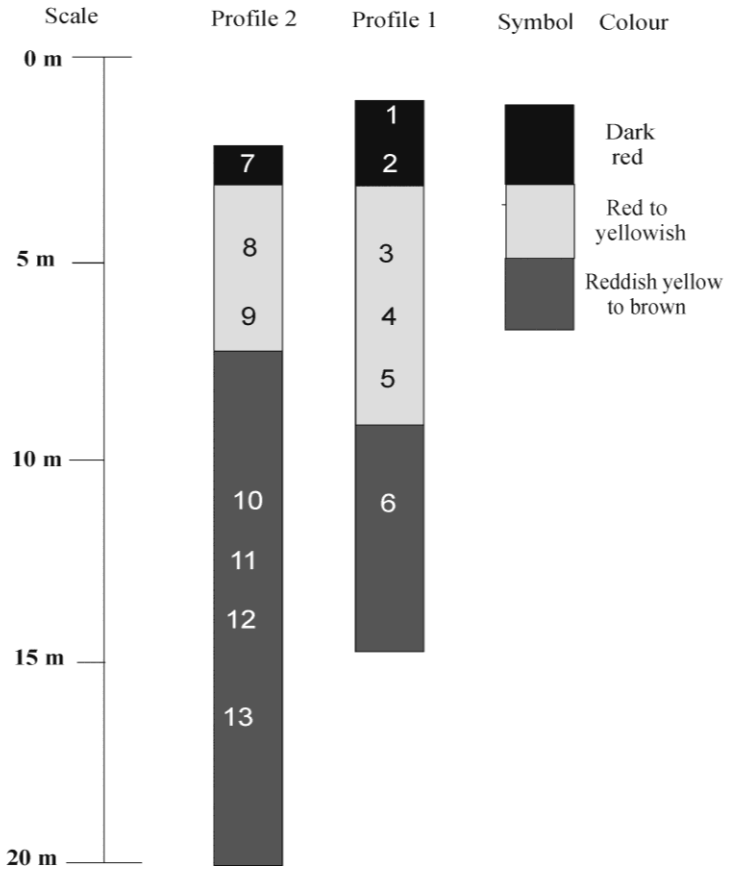

Figure 2.4 Vertical profiles from Duthuni Kaolin occurrence.

2.2 Clay genesis and classification: an overview

A clay material is any fine-grained, natural, earthy, argillaceous material (Grim, 1962). Clay is a rock term and is also used as a particle size term. The term clay has no generic significance because it is used for residual weathering products, hydrothermally altered products, and sedimentary deposits. As a particle size term, the size fraction comprised of the smallest particle is called the clay fraction (Murray, 2007). The Wentworth scale defines the clay grade as finer than 4 µm which is used by many engineers and soil scientist whereas clay scientists generally consider 2 µm as the upper limit of the clay size grade (Murray, 2007).

Grim (1968) summarized what he termed the clay mineral concept which stated that clays are composed essentially of a small group of extremely small crystalline particles of one or more members of a group of minerals the are commonly known as the clay minerals. The clay minerals are hydrous aluminium silicates and in some of these minerals, iron and magnesium substitute for the aluminium and in some, there are alkaline and alkaline earth elements present (Murray, 2007).

The clay mineral types are kaolin, smectite, palygorkite-sepiolite, which are sometimes referred to as hormites illite, chlorite, and mixed-layered clays (Martin-Vivaldi and Robertson, 1971). The properties of these clays are very different which are related to their structure and composition (Murray, 2000). A useful classification of the clay minerals was proposed and used in Grim in his book (1968), which is a basis for outlining the nomenclature and differences between the various clay minerals (Murray, 2007).

2.2.1 Geologic origin of clay minerals

Clays occur in many different geological environments: weathering crusts and soils, continental and marine sediments, volcanic deposits, geothermal fields, wallrock alteration produced by intrusion of plutonic rocks and hydrothermal fluids, and very low-grade metamorphic rocks. Clay minerals mostly form from pre-existing minerals, primarily from rock-forming silicates by transformation, and/or neoformation, where rocks are in contact with water, air, or steam. However, transportation, deposition, burial, and diagenesis of the weathered materials usually change the physico-chemical properties of clay minerals, and even influence their transformation into other clay minerals (Galan, 2006).

Clay formation and evolution are distinctive events in the geological history of a basin. Source area, transport, depositional environment of clays, and the transformation and diagenetic changes are fundamental for analysis of sedimentary basins (Galan, 2006).

2.2.1.1 Primary Kaolin

Kaolin deposits and occurrences could be primary or secondary depending on their genesis (Bailey, 1980; Dixon, 1989; Murray, 1999 a,b,c). hydrothermal, residual or mixed hydrothermal and residual are primary kaolins (Murray, 2007). They are formed in-situ, by the alteration of feldspar-rich, Al-rich rocks such as granites and rhyolites, parent minerals being feldspars and micas in particular muscovite (Murray, 1999 a,b). during alteration, all K must be released in solution to avoid formation of authigenic illite (Pickering and Murray, 1995). Kaolinisation can be due to surface weathering,

groundwater activity, or action of hydrothermal fluids. Dickite and nacrite are normally restricted to hydrothermal occurrences (Murray, 1998, 1999b).

Primary kaolin form from the transformation of primary aluminium silicates (especially feldspars) to clay minerals, through 1. Hydrothermal alteration (kaolin formed from granites), or 2. Normal weathering processes (sedimentary kaolin deposits). Hydrothermal clay bodies frequently have a zonal distribution, grading from sericite-rich portions in the centre through kaolinite-rich to smectite and chlorite-bearing zones near the outer margins. Kaolinite can form from most aluminous silicate host rocks, provided the environment is acidic, the moderate temperature and the alkalis and alkaline earths are removed as soon as the parent mineral breaks down leaving Al, Si, and sometimes Fe to accumulate as a residual material. However, studies have suggested that Fe normally mobilises at a later stage in the formation process (Horn et al., 1998).

2.2.1.2 Secondary kaolin

Secondary kaolins, also known as sedimentary kaolins, are genetically sedimentary; resulting from erosion and transportation of clay-size particles, which are mineralogically altered and deposieted as beds and lenses associated with other sedimentary rocks; in lacustrine, paludal, deltaic and lagoonal environments (Murray and Keller, 1993). Secondary kaolins could also be formed by the alteration of feldspathic arennites in sedimentary rocks such as arkose, resulting mostly from groundwater activity (Ekosse, 2001a).

Surficial weathering of acidic and basic igneous rocks often results in massive kaolin deposits. Controlling parameters include subtropical to tropical climate, good drainage, and a high rate of leaching of soluble elements such as K, Na, Mg, Ca, and Fe, which enrich the residue in Al and Si. These deposits are known as lateritic kaolin deposits and are currently forming in tropical areas. The decomposition of feldspar to form kaolin is also substantially accelerated by the presence of carbon dioxide or humic acids. Kaolin deposits are also known to have developed as a result of weathering of sediments, the process being very similar to the weathering of acid and basic igneous rocks (Horn et al., 1998).

2.3 Classification of clay minerals

The clay mineral types are kaolin, smectite, palygorkite-sepiolite, which are sometimes referred to as hormites illite, chlorite, and mixed-layered clays (Martin-Vivaldi and Robertson, 1971). The properties of these clays are very different which are related to their structure and composition (Murray, 2000a). A useful classification of the clay minerals was proposed and used in Grim in his book (1968), which is a basis for outlining the nomenclature and differences between the various clay minerals.

Murray (2007) bases his classification on the atomic structure of the clay minerals which consist of two basic units, an octahedral and tetrahedral sheet. The octahedral sheet is comprised of closely packed oxygen and hydroxyls in which aluminium, iron, and magnesium atoms are arranged in octahedral coordination. When aluminium with a positive valence of three is the cation present in the octahedral sheet, only two-thirds of the possible positions are filled to balance the charges. When only two-thirds of the positions are filled, the mineral is termed dioctahedral.

When magnesium with a positive charge of two is present, all three positions are filled to balance the structure and the mineral is termed trioctahedral (Murray, 2007). The second structural unit is the silica tetrahedral layer in which the silicon atom is equidistant from four oxygens or possibly hydroxyls arranged in the form of a tetrahedron with silicon atom in the centre. These tetrahedrons are arranged to form a hexagonal network repeated infinitely in two horizontal directions to form what is called silica tetrahedral sheet. The silica tetrahedral sheet and the octahedral sheet are joined by sharing the apical oxygens or hydroxyls to form what is termed the 1:1 clay mineral layer (*e.g.* kaolinite) or 2:1 clay mineral layer (*e.g.* illite) (Murray, 2007).

The structure and composition of the major industrial clays, (*i.e.* kaolins, smectites, and palygorkite-sepiolite), are different even though they are each comprised of octahedral and tetrahedral sheets as their basic building blocks (Murray, 2007). The arrangement and composition of the octahedral and tetrahedral sheets account for most of the differences in their physical and chemical properties (Murray, 2007).

2.3.1 Allophane

Allophane is a widely distributed clay mineral. Although characteristic of soils derived from volcanic ash, it has also been identified in Podzols and podzolised soils. Certain distinctive characteristics can be attributed to the spherical shape of allophane. The apparent specific surface is high and is decreased markedly on drying, thus enabling the external and internal surface areas and hence diameters of the spherules to be calculated. High phosphate retention is characteristics (Allbrook, 1985).

Very low bulk densities are found in perhumid climates. Shear strength of allophanic soils is generally less compared to non-allophanic soils. This is due to lower cohesion since friction is not altered. Both field moisture and liquid limits tend to be high. Wilting point expressed on a unit-clay basis is also high and like liquid limit it decreases markedly on drying. In very wet climates the wilting point may exceed 100% (Allbrook, 1985).

2.3.2 Kaolin

Kaolin is the name used in industry for a naturally occurring, white, fine-grained, non-plastic, earthy material, composed essentially of kaolin, which is a hydrated oxide of silica and alumina. However, industry applies the term kaolin to a wide range of clays, including those containing substantial quantities of minerals other than kaolinite itself (Horn et al., 1998).

Most kaolin deposits form as a result of the transformation of primary aluminium silicates (especially feldspars) to clay minerals, either through 1. Hydrothermal alteration (kaolin formed from granites), or 2. Normal weathering processes (sedimentary kaolin deposits). Hydrothermal clay bodies frequently have a zonal distribution, grading from sericite-rich portions in the centre through kaolinite-rich to smectite and chlorite-bearing zones near the outer margins. Kaolinite can form from most aluminous silicate host rocks, provided the environment is acidic, the moderate temperature and the alkalis and alkaline earths are removed as soon as the parent mineral breaks down leaving Al, Si, and sometimes Fe to accumulate as a residual material. However, studies have suggested that Fe normally mobilises at a later stage in the formation process (Horn et al., 1998).

Surficial weathering of acidic and basic igneous rocks often results in massive kaolin deposits. Controlling parameters include subtropical to tropical climate, good drainage, and a high rate of leaching of soluble elements such as K, Na, Mg, Ca, and Fe, which enrich the residue in Al and Si. These deposits are known as lateritic kaolin deposits and are currently forming in tropical areas. The decomposition of feldspar to form kaolin is also substantially accelerated by the presence of carbon dioxide or humic acids. Kaolin deposits are also known to have developed as a result of weathering of sediments, the process being very similar to the weathering of acid and basic igneous rocks (Horn et al., 1998).

The basic kaolin mineral structure comprising the minerals kaolinite, dickite, nacrite, and halloysite is a layer of a single tetrahedral sheet and a single octahedral sheet (Murray, 2007). These two sheets are combined to form a unit in which the tips of the silica tetrahedrons are joined with octahedral sheet. All of the apical oxygens of the silica tetrahedrons point in the same direction so that these oxygens and/or hydroxyls, which may be present to balance the charges, are shared by silicons in the tetrahedral sheet and the aluminium in the octahedral sheet. The structural formula for kaolinite is $Al_4Si_4O_{10}(OH)_8$ and the theoretical chemical composition is Si_2, 46.54%; Al_2O_3, 39.50%; and H_2O, 13.96%.

Only two-thirds of the octahedral positions are filled by an aluminium atom. The aluminium atoms are surrounded by four oxygens and eight hydroxyls. The charges in the kaolinite structure are balanced. The minerals of the kaolin group, kaolinite, dickite, nacrite, and halloysite consist of the so-called 1:1 layers of combined octahedral and tetrahedral sheets, which are continuous in the a- and b- axis directions and are stacked one above

the other in the c-axis direction. The differences in the kaolin minerals are the manner in which the unit layers are stacked above each other. The thickness of the unit layer is 7.13A (Murray, 2007).

In dickite, the unit cell consists of two unit layers and in nacrite, six unit layers. Halloysite occurs in two forms: one hydrated, in which there is a layer of water molecules between the layers, and one dehydrated. The hydrated form has a basal spacing of 10A and the dehydrated form, 7.2A. The shape of halloysite is elongate tubes whereas the shape of kaolinite is pseudo-hexagonal plates and stacks. The International Nomenclature Committee has recommended the terms 7A halloysite and 10A halloysite to designate the two forms (Murray, 2007).

The elongate tubular form according to Bates et al. (1950) is made up of overlapping curved sheets of the kaolinite type. The curvature develops in 10A halloysite because of the irregular stacking of the layers and the interlayer of water molecules, which cause a weak bond between the layers. The tendency to curve is caused by a slight difference in dimension of the silicon tetrahedral sheet and the alumina octahedral sheet.

Kaolinite (one of the common members of the kaolin group) is a clay mineral, with the chemical composition $Al_2Si_2O_5(OH)_4$. It is a layered silicate mineral, with one tetrahedral sheet of silica (SiO_4) linked through oxygen atoms to one octahedral sheet of alumina octahedral (Lackovic et al., 2003; Srivastava et al., 2005). Kaolin is the weathering product of feldspars. It has a white, powdery appearance. Since kaolin clay mineral is electrically balanced, its ability of adsorb ions is less than that of other clay minerals. Kaolin has octahedral layer similar to the gibbsite structure (Murray, 1994, Murray 2007).

The water absorption and expansion of Kaolinite is low. Thus, kaolinite is the preferred type of clay for industrial application (Murray, 1994, Murray 2007). Kaolin has a low shrink–swell capacity and a low cation-exchange capacity. It is a soft, earthy, usually white, mineral (dioctahedral phyllosilicate clay), produced by the chemical weathering of aluminium silicate minerals like feldspar. In many parts of the world it is coloured pink-orange-red by iron oxide, giving it a distinct rust hue. Lighter concentrations yield white, yellow, or light orange colours. Commercial grades of kaolin are supplied and transported as dry powder, semi-dry noodle or as liquid slurry.

2.3.3 Smectite

The major smectite minerals are sodium montmorillonite, calcium montmorillonite, saponite (Magnesium montmorillonite), nontronite (iron montmorillonite), hectorite (lithium montmorillonite), and beidellite (aluminium montmorillonite). The theoretical formula is $Si_8Al_4O_{20}(OH)4$. NH_2O (interlayer) and the theoretical composition without the interlayer material is SiO_2, 66.7%; Al_2O_3, 28.3%; and H_2O, 5%. If the octahedral positions are filed by aluminium, the smectite mineral is beidellite; if filled by magnesium, the mineral is saponite; and if by iron, the mineral is nontronite. The most common smectite mineral is calcium montmorillonite, which means that the layer charge deficiency is balanced by the interlayer cation calcium and water. The smectite mineral particles are very small and because of this, the X-ray diffraction data are sometimes difficult to analyse (Murray, 2007).

Smectite is the name used for a group of phyllosilicate mineral species, the most important of which are montmorillonite, beidellite, nontronite, saponite and hectorite.

These and several other less common species are differentiated by variations in chemical composition involving substitutions of Al for Si in tetrahedral cation sites and Al, Fe, Mg and Li in octahedral cation sites (Murray, 1994; Murray 2007). Smectite clays have a variable net negative charge, which is balanced by Na, Ca, Mg and, or, H adsorbed externally on interlamellar surfaces. The structure, chemical composition, exchangeable ion type and small crystal size of smectite clays are responsible for several unique properties, including a large chemically active surface area, a high cation exchange capacity, interlamellar surfaces having unusual hydration characteristics, and sometimes the ability to modify strongly the flow behaviour of liquids. In terms of major industrial and chemical uses, natural smectite clays can be divided into three categories, Na smectites, Ca-Mg smectites and Fuller's or acid earths.

Smectite clay minerals also occur as a weathering product of mafic silicates. They are stable in arid, semi-arid, or temperate climates. Montmorillonite is the most common member of this group. They belong to a family of dioctohedral layer, lattic silicate with a 2:1 structure. The 2:1 layer in smectites are held together by van der Waals bonds and weak cation-to-oxygen linkages (Murray, 1994; Murray 2007). The presence of exchangeable cations located between water molecules in the interlayer allows for expansion of the crystal lattice as the mineral hydrates. When the mineral is saturated with water, the basal spacing between layers can approach 2 nm, while under dry conditions, the basal spacing may be reduced (Murray 2007). The expansion and contraction trait common with smectites is often referred to as shrink-swell potential. This expansion behaviour in smectites is problematic to engineers due to the propensity for

crack formation and general instability of the soil surface. This equally has considerable effects on the ceramic exploitation of smectite-rich raw materials (Diko et al, 2011).

2.3.4 Vermiculite

Vermiculite is the name given to a group of platy micaceous minerals of viable composition, with the chemical formula $(Mg,Fe,Al)_3(Al,Si)_4O_{10}(OH)_2.4H_2O$. They are hydrous magnesium-iron aluminosilicates and have the unique property of exfoliation, i.e. expansion perpendicular to the cleavage plane when heated rapidly. Vermiculite may be formed by the weathering, or hydrothermal alteration of phlogopite, with the resultant hydration and loss of an alkali. It is commonly associated with ultrabasic rocks such as serpentinite and pyroxenite (Wilson, 1998).

2.3.5 Illite

Illite is a clay mineral, which was named by Grim et al. (1937). The size, charge, coordination number of potassium is such that it fits snugly in the hexagonal ring of oxygens of the adjacent silica tetrahedral sheets. A simple way of thinking about illite is that it is a potassium smectite. Illite is commonly associated with many kaolins and smectites (Murray, 2007).

Illite is anon expandable clay crystalline mineral. It is a secondary mineral precipitate phyllosillicate or layered aluminosilicate. Its structure is 2:1 clay silica tetrahedron-alumina octahedron-silica tetrahedron layers (Murray 2007). Because of possible charge imbalance, Ca and Mg can also sometimes substitute for K. The K, Ca, or Mg interlayer cations prevent the entrance of H_2O into the structure. Thus, the illite clays are non-

expanding clays but are often present as mixed-layer clays with montmorillonite and/or chlorite. Illite is the weathering product of feldspars and felsic silicates Murray 2007), and has a three-sheet layer structure, one octahedral sheet sandwiched between two silica tetrahedral sheets (Murray 1994). The structure of mica (a coarse-grained rock-forming mineral) is essentially the same as the structure of illite, except that mica has less substitution in the octahedral layer. The Illite clays also have a structure similar to that of Muscovite, but are typically deficient in alkalies, with less Al substitution for Si.

2.3.6 Chlorite Minerals

Chlorite is commonly present in shales and in underclays associated with coal seams. Clay mineral chlorite differ from well-crystallized chlorites in that there is random stacking of the layers and also some hydration. Chlorite has been identified in many sandstones as coatings on quartz grains that appear as rosettes. Chlorite is generally intimately intermixed with other clay minerals (Murray, 2007).

Chlorites are a group of phyllosilicate minerals that exhibit a basic 2:1 layer structure similar to that of pyrophyllite, but with an interlayer brucite- or gibbsite-like sheet, which forms a 2:1:1 structural arrangement (Murray, 1994; Murray 2007). The typical general formula is: $(Mg,Fe)_3(Si,Al)_4O_{10}(OH)_2 \cdot (Mg,Fe)_3(OH)_6$. This formula emphasises the structure of the group. While, a typical formula for the interlayer sheet is (MgFeAl)(OH). However, a variety of cation species may exist in these brucite or gibbsite-like islands that contribute to a large number of mineral species within this group (Murray 2007). There is no water adsorption within the interlayer space; thus, chlorites are considered non-expansive minerals (Murray, 1994; Murray 2007). Their cation exchange capacity and

surface charge densities are low. The negative charge generated by isomorphous substitution is compensated by brucite (Mg Hydroxide) of ten positive charges due to isomorphous exchange of Mg^{2+} by Al^{3+} (Murray, 1994, Murray, 2007). This clay mineral is the weathering product of mafic silicates (silicates of magnesium and iron) such as Olivine, Labradorite and Biotite and is stable in cool, dry, or temperate climates.

2.3.7 Palygorskite and sepiolite

The term palygorkite and attapulgite are synonymous, but the international Nomenclature Committee has declared that the preferred name is Polygorkite. However, the term attapulgite is still used, particularlyby those that mine, process, and use this clay mineral. In this research, the term palygorskite will be used, but users should be aware that attapulgite is the same mineral. Palygorskite is a crystalline hydrated magnesium aluminum silicate with unique three-dimensional structure and has a fibrous morphology. Their unique morphology and structure provide a potential for diverse applications (Murray 2007).

This mineral actually resembles the amphiboles more than it does clay minerals but has a special property that smectite lacks - as a drilling fluid, as it is stable in saltwater environments. When drilling for offshore oil, conventional drilling mud falls apart in the presence of saltwater. Palygorskite is used as a drilling mud in these instances. Palygorskite and sepiolite are 2:1-layer silicates. The tetrahedral sheets are linked infinitely in two dimensions. However, they are structurally different from other clay minerals in that the octahedral sheets are continuous in only one dimension and the

tetrahedral sheets are divided into ribbons by the periodic inversion of rows of tetrahedrons (Murray 2007).

2.3.8 Mixed-layer clay

Sometimes known as common clays can be seat earths (underclays), shales, lacustrine clays, soils, and other clay-rich materials (Murray, 1994). Usually, the clay mineral composition of these materials is mixed. Mixed-layered or interstratified clay minerals usually contain two components such as illite and smectite. Most commonly, the layers are randomly ordered, but can be regularly ordered (Murray, 2007). This regularly ordered illite-smectite is called rectorite (Mapuna et al., 2023; Fadil-Djenabou et al., 2023)

The physical and chemicals properties are very diverse, so these common clays are utilized for specific ens uses. The physical properties that are normally important relate to their use in the manufacture of structural clay products such as bricks and tiles. These properties are plasticity, green strength, dry strength, dry and fire shrinkage, fired color, fired strength, vitrification range, and fired density. Many shales and seat earth (underclays) are suitable for making structural clay products (Murray, 2007).

Certain low-grade refractories can be made from some underclays of fireclays. These clays are generally mixtures of predominantly kaolinite, along with minor quantities of illite and /or chlorite. In addition to those physical properties needed for a common brick layer, the pyrometric cone equivalent (PCE) is important, along with the ability to withstand moderately high temperatures without melting or fusing. Refractory bricks are classified as low, medium, high, and super duty (Murray, 2007). Some common clays or shales are

used to make lightweight aggregate (Murray and Smith, 1958; Mason, 1994). Others can be used as a raw material in the mix to make cement.

2.4 Kaolin physico-chemistry, mineralogy and geochemistry

2.4.1 Physico-chemical properties of kaolin

The properties of clay that are of interest to ceramics industry are its plasticity which facilitates the shape of the body, chemistry, mineral composition, thermal property, colour, refractoriness and mechanical strength after firing (Baccour et al., 2009; Burst, 1991).

The most important properties that kaolin and ball clay impart to ceramics are plasticity, green strength, dry strength, fired strength, color, refractoriness, ease of casting in sanitary ware, low to zero absorption of water, and controlled shrinkage (Murray, 2007). Shrinkage is an important property because ceramic articles undergo shrinkage at two different points in the manufacturing sequence. During drying, the article will shrink in varying amounts depending on the composition and the percentage of water present. During firing, the ceramic article will further shrink. Therefore, it is important to know both the drying and firing shrinkage (Murray, 2007).

Linear and volume shrinkage can both be measured, although linear shrinkage is more commonly reported (Jones and Bernard, 1972). In unfired body, both the water of plasticity and shrinkage generally decrease as the particle size increases. In the fired body, the firing shrinkage and water absorption generally decrease, whereas the modulus of rupture (MOR) and fired whiteness generally increase as the particle size increase (Fadil-Djenabou et al., 2023, Mapuna et al., 2023).

Plasticity is defined as the property of a material which permits it to be deformed under stress without rupturing and to retain the shape produced after the stress is removed (Grim, 1962). The measurement of plasticity has been difficult to determine qualitatively. One is to determine the amount of water necessary to develop optimum plasticity or the range of water content in which plasticity of the material is demonstrated (Murray, 2007).

The lower value, called the plastic limit, and the higher limit, called the liquid limit, is the plastic index (Diko and Ligege, 2020). A second method is to determine the amount of penetration of a needle or some type of plunger into a plastic mass of clay under a given load or rate loading (Whittemore, 1935). Another way is the stress necessary to deform the clay and the maximum deformation the clay will undergo before rupture. Bloor (1957) presented a critical review of plasticity. A Brabender plastigraph can be used to measure the stress limits mentioned above. Carty et al. (2000) described a high-pressure annulus shear cell or HPASC, as a new plasticity characterization technique.

Green strength is measured as the transverse breaking strength of a test bar suspended on two narrow supports in pounds per square inch or kilograms per square centimetre (Murray, 2007). Green strength has to be adequate for the piece to be handled without bending or breaking. Ball clays, which are finer in particle size than most kaolins, have a higher green strength (Holderidge, 1956).

Drying shrinkage is the reduction in size, measured either in length or volume that takes place when the clay piece is dried to drive off the pore water and adsorbed water (Murray, 2007). The drying shrinkage is expressed in percent reduction in size based on the size after drying. In the laboratory, the measurement is made on a test bar after drying for a minimum of 5 h at 105ºC. The drying shrinkage is related to the water of plasticity. It

increases as the water of plasticity increases and also increases as the particle size decreases. Dry strength is the transverse breaking strength of a test bar that has been dried to remove all the pores and adsorbed water. The dry strength of kaolins and ball clays is greater than their green strength. Dry strength is closely related to particle size which indeed is a major controlling factor (Murray, 2007).

2.4.2 Mineralogical properties of kaolin

Konta (1995) indicated that industrial/technology properties of raw kaolin are dependent on the properties of the clay minerals present, total mineral composition, and degree of consolidation. The mineral contents and geology affect kaolin quality (Hinckley, 1963), applications (Ekosse and Mulaba - Bafibiandi, 2006). In this regard, understanding the mineralogy of any given kaolin is crucial in determining its possible applications. Kaolin deposits and occurrences in Africa were mineralogically dominated by kaolinite. Illite and smectite were present in slightly above 20 different kaolin deposits and occurrences. Other clay minerals, to a lesser extent, reported in African kaolins included chlorite, hydromica, muscovite, palygorskite, pyrophyllite and vermiculite.

These clay minerals were also reported in several well-known kaolin in USA, Rio Capim kaolin in Brazil, and the Maoming kaolin in China (Murray and Keller, 1993; Yuan and Murray, 1993; Murray et al., 2007). Whereas East African kaolin contained more of other clay minerals than those in the other continental geographic regions, those from central Africa had the least variety of other clay minerals. Southern and West Africa had more kaolin with smectite than those from other regions.

Non clay minerals which include over 27 other minerals occurred as part of the mineral assemblages for Africa kaolins. These minerals included fe-rich minerals (goethite, haematite, limonite, siderite and pyrite) which influence kaolin colour Ca- bearing minerals (calcite, aragonite and dolomite) which affect kaolin brightness, and quartz, feldspar and mica that affect particle size distribution of particles within a kaolin deposit or occurrence. Most of the other non-clay minerals were very sparsely represented in few deposits in the regions.

Quartz occurred in several deposits even in the fractionated <2 μm in all the regions. The <2 μm in all the fraction of some the kaolin from Serule, Botswana; and those from Alkeleri area (Beni, Cheledi and Gwaram) in Nigeria. Scanning electron microscopy of some African kaolins depicted morphologies of kaolinite particles which were desirable for a wide range of industrial applications. The scanning electron photomicrographs of makoro and Kgwagwe in Botswana and Beni in Nigeria.

The morphologies of the clay particles of these kaolins reflected shapes of particles required for different functional applications (Ekosse and Shemang, 2002; Ekosse and Mulaba-Bafubiandi, 2003 Shemang et al., 2007).

Accessory minerals (both clay and non-clay minerals) in most kaolin deposits and occurrences in the world include muscovite, Illite, biotite, rutile, anatase, tourmaline, goethite, ilmenite, magnetite, quartz, and smectite. Kaolin minerals could be interstratified with either illitic or smectitic clay minerals (Tsolis-Katagas and Mavronichi, 1989). The mineral assemblages for African kaolin were similar to those from other parts of the world. Minerals impurities in kaolin determine beneficiation processes to be used in improving

kaolinite grade for its suitability to a given application (Murray, 1980, 1999). Smectites, alunite and halloysite increase viscosity, and the later also lower the opacity of hiding power, whereas quartz and/or cristobalite causes high abrasion effect on the applied finished product (Murray, 1980). Pyrite and goethite reduce the brightness of the finished product.

2.4.3 Geochemical properties of kaolin

The chemical formula of the major kaolin mineral kaolinite is $Al_2Si_2O_5(OH)_4$ and it consists of 39.8% mass Al_2O_3, 46.3% mass SiO_2, and 13.9% mass H2O. The SiO_2/Al_2O_3 value for theoretical kaolinite is 1.16, both Cornwall Kaolinite and Maoming Kaolinite is 1.24, whereas Georgia Kaolinite is 1.18 (Murray and Killer, 1993; Yuan and Murray, 1993). This ratio for whole kaolin from Central Africa ranged between 1 and 3.8, 1-7 for East Africa, 1-35 for North Africa, 1-3, 1 for Southern Africa and 1-5.1 for West Africa.

In most industrial applications of kaolin, it is desirable for the mineral to have a chemical composition, which is comparatively closer to its theoretical value. However, because kaolin is usually associated with other minerals, it is rare to find it pure in nature. Kaolin chemistry is affected by mineral contamination, usually present in the form of Fe^{3+}, Fe^{2+}, Mg^{2+}, Ca^{2+}, Na^{+}, and $PO4^{3-}$ (Christidis and Scott, 1997; 1998).

Kaolin could be either surfacially or structurally contaminated (Cases et al., 1982; Tsolis-Katagas and Mavronichi, 1989; Buhmann, 1994). Surface impurities, which usually adhere to kaolin particles, can easily be removed through washing. Isomorphous substitution of elements for Al in the octahedral sheet of kaolinite results in structural impurities of Fe, Ti and Mn (Cases et al., 1982; Michailidis and Tsirambides, 1986;

Ekosse, 2000). For most applications of kaolins, the concentrations of major elements such as Mn and Fe should not exceed 5 ppm (Ekosse, 2000) Ions that have become part of the mineral structure are difficult and expensive to get rid of.

2.5 Kaolin as raw ceramic materials

Ceramics includes a wide range of products in which kaolins are utilized. These include dinnerware, sanitaryware, tile, electrical porcelain, pottery, and refractories, kaolins and ball clays, which are kaolinitic clays, are both used as major ingredients in many ceramic products (Murray, 2007). The term ceramic refers to the manufacture of products from earthen materials by the application of high temperature (Grim, 1962).

Ceramics historically goes back to prehistoric times when early man used earthenware in cooking (Murray, 2007). He learns that he could form shapes with plastic clays and that heat would fix the shape and make them stable in water. Through time, with the development of modern science, ceramic art has become an engineering profession.

The ceramic properties of clay materials are variable depending on the clay mineral composition and such properties as particle size distribution, presence of organic material, and the non-clay mineral composition (Murray, 2007). The clay mineral composition is the most important factor determining ceramic properties (Murray, 2007). Kaolinite is the most important clay mineral used in ceramic applications because of its physical and chemical properties that are imported to ceramic processing and finished products (Murray, 2007).

The most important properties that kaolin and ball clay impart to ceramics are plasticity, green strength, dry strength, fired strength, color, refractoriness, ease of casting in

sanitaryware, low to zero absorption of water, and controlled shrinkage (Murray, 2007). Shrinkage is an important property because ceramic articles undergo shrinkage at two different points in the manufacturing sequence. During drying, the article will shrink in varying amounts depending on the composition and the percentage of water present. During firing, the ceramic article will further shrink. Therefore, it is important to know both the drying and firing shrinkage (Murray, 2007).

Linear and volume shrinkage can both be measured, although linear shrinkage is more commonly reported (Jones and Bernard, 1972). In unfired body, both the water of plasticity and shrinkage generally decrease as the particle size increases. In the fired body, the firing shrinkage and water absorption generally decrease, whereas the modulus of rupture (MOR) and fired whiteness generally increase as the particle size increase (Mapuna et al., 2023; Fadil-Djenabou et al., 2023).

Plasticity is defined as the property of a material which permits it to be deformed under stress without rupturing and to retain the shape produced after the stress is removed (Grim, 1962). The measurement of plasticity has been difficult to determine qualitatively (Murray, 2007). One is to determine the amount of water necessary to develop optimum plasticity or the range of water content in which plasticity of the material is demonstrated. Atterberg (1911) proposed that the lower value, called the plastic limit, and the higher limit, called the liquid limit, is the plastic index.

A second method is to determine the amount of penetration of a needle or some type of plunger into a plastic mass of clay under a given load or rate loading (Whittemore, 1935). Another way is the stress necessary to deform the clay and the maximum deformation the clay will undergo before rupture. Bloor (1957) presented a critical review of plasticity.

A Brabender plastigraph can be used to measure the stress limits mentioned above. Carty et al. (2000) described a high pressure annulus shear cell or HPASC, as a new plasticity characterization technique.

Green strength is measured as the transverse breaking strength of a test bar suspended on two narrow supports in pounds per square inch or kilograms per square centimetre (Murray, 2007). Green strength has to be adequate for the piece to be handled without bending or breaking. Ball clays, which are finer in particle size than most kaolins, have a higher green strength (Holderidge, 1956).

Drying shrinkage is the reduction in size, measured either in length or volume that takes place when the clay piece is dried to drive off the pore water and adsorbed water (Murray, 2007). The drying shrinkage is expressed in percent reduction in size based on the size after drying. In the laboratory, the measurement is made on a test bar after drying for a minimum of 5 h at 105ºC. The drying shrinkage is related to the water of plasticity. It increases as the water of plasticity increases and also increases as the particle size decreases. Dry strength is the transverse breaking strength of a test bar that has been dried to remove all the pores and adsorbed water. The dry strength of kaolins and ball clays is greater than their green strength. Dry strength is closely related to particle size which indeed is a major controlling factor (Murray, 2007).

The fired properties of kaolins are most important in determining the ceramic application for a particular kaolin product (Murray, 2007). It should be understood that the non-clay mineral components such as quartz, feldspar, and other mineral additives play an important role in determining the firing characteristics. If organic material is present as it is in ball clays, oxidation to destroy the organic materials begins at a temperature of about

300ºC and is completed at a temperature of about 500ºC. At a temperature between 550 and 600ºC, kaolinite is dehydroxylated and lattice structure of kaolinite becomes amorphous even though the particle shape is largely retained. This amorphous arrangement of the silica and alumina is retained until a temperature of about 980ºC is reached. At that temperature, the amorphous mixture of silica and alumina in metakaolin combines to form a new phase. When this new phase forms, an exothermic reaction takes place (Murray, 2007).

There is some dispute about the phase that is formed at this temperature, but most believe the exothermic reaction is caused by the nucleation of mullite (Johns, 1953). Further heating to a temperature of 1200ºC results in larger crystallites of mullite, which Wahl (1958) calls secondary mullite. Kaolinite fuses at 1650-1775ºC (Norton, 1968). The fired color of kaolinite is white or near-white. The MOR of fired kaolinite is very high compared to the MOR of the dried counterparts. The MOR reported for fired pieces is generally a blend of 50% fine silica and 50% kaolin clay. The MOR ranges from 300 to 900 psi depending largely on the particle size of the kaolin clay (Murray, 2007).

Casting rate is important in the manufacture of sanitaryware (Murray, 2007). Fine-grained bodies cast more slowly than coarse ones. The viscosity of a slip must be carefully controlled because if it is too viscous, the slip will not properly fillthe mold or drain cleanly and relatively fast. Therefore, viscosity is measured on kaolins and ball clays that are used in the casting process. Halloyside is used as an additive in the manufacture of high quality dinnerware (Murray, 2007). The addition of 5-10% by weight in the body provides high fired brightness and increased translucency, both of which are desirable properties of dinnerware.

The use of kaolins and ball clays in refractories began in the early 1800s in New Jersey (Murray, 2007). Refractory clays are used primarily to make fire bricks and blocks of many shapes, insulating bricks, saggers, refractory mortars and mixes, monolithic and castable materials, ramming and air gun mixes, and other refractory products. The specifications for refractory clays are as many as the different uses. Resistance heat is the most essential property and pyrometric cones are used to indicate the heat duty required. The pyrometric cone measures the combined effects of temperature and time (Norton, 1968).

The cones consist of series of standardized unfired ceramic compositions moulded into the shape of triangular pyramids. The samples of kaolin, ball clay, or refractory composition is moulded into the standard cone shape and is heated along with standard cones so that the end point can be determined in terms of an equivalent cone number. Refractory bricks are classed as low, medium, high and super duty (Murray, 2007). The Pyrometric Cone Equivalent (PCE) values of low duty are from 15 to 29, medium duty from 29 to 31, high duty from 31 to 33, and super duty above 33. Flint clays are very refractory but are non-plastic so are mixed with plastic kaolin and/or ball clays to provide the plasticity needed to form the piece and maintain its shape (Murray, 2007).

2.6 Effects of heat treatment on ceramic properties of kaolin

The fired properties of kaolins are most important in determining the ceramic application for a particular kaolin product (Murray, 2007). The non-clay mineral components such as quartz, feldspar, and other mineral additives play an important role in determining the firing characteristics. If organic material is present as it is in ball clays, oxidation to destroy

the organic materials begins at a temperature of about 300ºC and is completed at a temperature of about 500ºC.

At a temperature between 550 and 600ºC, kaolinite is dehydroxylated and lattice structure of kaolinite becomes amorphous even though the particle shape is largely retained. This amorphous arrangement of the silica and alumina is retained until a temperature of about 980ºC is reached. At that temperature, the amorphous mixture of silica and alumina in metakaolin combines to form a new phase. When this new phase forms, an exothermic reaction takes place (Murray, 2007).

There is some dispute about the phase that is formed at this temperature, but most believe the exothermic reaction is caused by the nucleation of mullite (Johns, 1953). Further heating to a temperature of 1200ºC results in larger crystallites of mullite, which Wahl (1958) calls secondary mullite. Kaolinite fuses at 1650-1775ºC (Norton, 1968). The fired color of kaolinite is white or near-white. The MOR of fired kaolinite is very high compared to the MOR of the dried counterparts. The MOR reported for fired pieces is generally a blend of 50% fine silica and 50% kaolin clay. The MOR ranges from 300 to 900 psi depending largely on the particle size of the kaolin clay (Murray, 2007).

Casting rate is important in the manufacture of sanitaryware (Murray, 2007). Fine-grained bodies cast more slowly than coarse ones. The viscosity of a slip must be carefully controlled because if it is too viscous, the slip will not properly fillthe mold or drain cleanly and relatively fast. Therefore, viscosity is measured on kaolins and ball clays that are used in the casting process. Halloyside is used as an additive in the manufacture of high quality dinnerware (Murray, 2007). The addition of 5-10% by weight in the body provides

high fired brightness and increased translucency, both of which are desirable properties of dinnerware.

The use of kaolins and ball clays in refractories began in the early 1800s in New Jersey (Murray, 2007). Refractory clays are used primarily to make fire bricks and blocks of many shapes, insulating bricks, saggers, refractory mortars and mixes, monolithic and castable materials, ramming and air gun mixes, and other refractory products. The specifications for refractory clays are as many as the different uses. Resistance heat is the most essential property and pyrometric cones are used to indicate the heat duty required. The pyrometric cone measures the combined effects of temperature and time (Norton, 1968).

The cones consist of series of standardized unfired ceramic compositions moulded into the shape of triangular pyramids. The samples of kaolin, ball clay, or refractory composition is moulded into the standard cone shape and is heated along with standard cones so that the end point can be determined in terms of an equivalent cone number. Refractory bricks are classed as low, medium, high and super duty (Murray, 2007). The Pyrometric Cone Equivalent (PCE) values of low duty are from 15 to 29, medium duty from 29 to 31, high duty from 31 to 33, and super duty above 33. Flint clays are very refractory but are non-plastic so are mixed with plastic kaolin and/or ball clays to provide the plasticity needed to form the piece and maintain its shape (Murray, 2007).

2.7. Technological controls on ceramic potentials of kaolin

The technological properties of clay materials are largely depended on several factors. The interdependence of mineralogy, chemical composition, particle size distribution, texture, and surface activity with their technological behaviour in ceramic production.

Plasticity is strictly dependent on surface activity, < 2 μm fraction and expandable clay minerals; slip rheology is affected by soluble salts and expandable clay minerals, but also by high specific surface or tubular halloysite. Kaolinite/halloysite play an opposite role versus smectite/interstratified I/S in slip casting and tile pressing: the former allow faster casting rates, while the latter improve powder flowability and mechanical strength. Kaolinite and quartz are beneficial for drying behaviour while high surface activity or expandable clay minerals increase significantly drying sensitivity. According to Dondi et al (2008) firing behaviour is mainly affected by minor components supplying “fluxing” (i.e., iron, alkali and alkaline earth).

CHAPTER THREE: MATERIALS AND METHODS

3.1 Field work

3.1.1 Sampling

Two representative samples (D1 and D2) were collected from the main excavation pit. The pit was divided into two horizons based on colour – red to reddish brown (D1), and cream to yellowish brown (D2). Clay samples were obtained from each sub-unit within the predefined horizons to produce a homogenous mixture of 50 kg for a series of laboratory analysis including thermal behaviour. Representatives were ensured by collecting the samples from two main heterogeneous kaolin bearing layers within the respective excavation pits. Heterogeneity between layers was defined by differences in colour, texture and mineralogy (Diko, 2012).

3.2 Analytical procedures

Composite samples of natural clay from two outcrops each labelled D1 and D2 from the study area (about 50 kg each) were analyzed for particle size distribution (PSD), colour, Atterberg limits (liquid limit, plastic limit, plasticity index and clay activity), mineralogical and chemical composition, and technological properties; weight loss (WL), bulk density (BD), water absorption (WA), linear shrinkage (LS) and flexural strength (FS).

3.2.1 Physicochemical analyses

The analyses were conducted to determine but not limited particle size, colour, and Atterberg limits.

3.2.1.1 Particle size distribution

Particle size distribution (PSD) was determined by laser diffraction technique. Laser diffraction-based particle size analysis relies on the fact that particles passing through a laser beam will scatter light at an angle that is directly related to their size. As particle size decreases, the observed scattering angle increases logarithmically. Scattering intensity is also dependent on particle size, diminishing with particle volume. Large particles therefore scatter light at narrow angles with high intensity, whereas small particles scatter at wider angles but with low intensity. Particle size analysis by laser diffraction was performed with a Saturn DigiSizer 5200. The samples were dispersed in a water medium to form a suspension of 0.00139 wt % solids and drawn into the size analyser at a flow rate of 12.0 L/min and circulation time of 120 seconds.

3.2.1.2 Colour

Colour was determined using Munsell Soil Colour Book (Diko et al., 2014). According to Munsell classification scheme, full attributes of colour include hue, value and chroma. For colour determination the raw samples were aerated for 24 h. Using a spatula, clayey aggregates were mounted on white cardboard sheets. The hue/value/chroma and colour of the mounted samples were obtained by visually comparing them to those of standard soils recorded in the Munsell Soil Colour Book.

3.2.1.3 Atterberg limits

Atterberg limits were performed on the < 63 µm fraction samples using the Cassagrande apparatus (Diko et al., 2014). For LL determination, 40 g of previously prepared fine

mortar was spread in a cup (maximum thickness =1 cm) and divided by a standard axial groove. The LL was expressed as a percentage by weight of the mortar after drying in an oven at 105 °C, at which the groove closes over a length of 1 cm under the influence of 25 blows. The blows were produced by allowing the cup to drop from a height of 1 cm onto a hard surface.

To determine the PL, 10 g of the fine mortar was used. Using the palm, the mortar was rolled on a flat surface until the tread of fine mortar broke into sections of between 1 cm and 2 cm long, after being reduced to a diameter of 3 mm. The PL was expressed as a percentage by weight after oven drying at 105 °C. The PI was obtained from the arithmetic difference between LL and PL, whereas CA was calculated from the following expression:

$$CA = PI/clay\ wt\ \% \quad (1)$$

3.2.2 Mineralogical analyses

3.2.2.1 X-Ray diffraction

X-ray diffractometry was used for mineral identification. Prior to analysis, the samples were air-dried and gently ground with the aid of mortar and pestle into powdery form. The ground samples were loaded in sample holders and mounted on a BRUKER D8 Advance diffractometer equipped with a LYNXEYE detector and a Ni-filter. Powder mounts were scanned from 2 to 70° 2θ CuK (λ=1.54060) radiation at a speed of 0.05° 2θ steps size per second and generator settings of 40 kV and 40 mA. Overnight glycolation (<24 h) test was performed to distinguish smectites from vermiculite (Yongue-Fouateu et al 2016).

Phase identification was based on BRUKER DIFFRAC Plus-EVA evaluation program. Phase concentrations were determined as semi quantitative estimates (with accuracy ±

5%) using Reference Intensity Ratio (RIR) method and relative peak heights/areas proportions (Ekosse et al 2017).

3.2.2.2 Thermal analysis

For thermal analyses the following tests were conducted; differential scanning calorimetry (DSC) and thermogravimetry (TG). The DSC/TG thermo-analytical methods focus on the measurement of difference in temperature and masses between samples and reference materials while both are subjected to a controlled temperature program. The DSC technique involves heating the kaolin samples and observing endothermic and exothermic reactions occurring. These reactions are recorded by a differential thermal analyzer (Ekosse, 2008). The TG analysis on the other hand monitors the mass of the kaolin samples when subjected to a controlled temperature program (Ekosse, 2008). The principle of operation is based on the equation of Kissinger (1957). Peak temperature values are obtained as follows;

$$\ln (\Theta T_m^{-2}) = C - E (RT_m^{-1}) \quad (6)$$

Where: Θ = Heating rate, T_m = Peak temperature, C = Intergrating constant, E = Activation energy and R = Gas constant

Thermal analysis was conducted with a TA instrument SDT Q600 TGA-DSC analyser (University of Kwa-Zulu Natal). Calcined Al_2O_3 served as the insert standard, while measurements were performed with 20 mg of samples, heated in air at 10°C/min, from 25°C to 1100°C as discussed in Njoya et al. (2006).

3.2.2.3 Fourier transform infrared spectrophotometry

Fourier transform infrared (FTIR) spectrophotometry is an alternative method for determining qualitative/quantitative mineralogy. The mineralogy can be inferred from the FTIR spectrum given that minerals exhibit most of their fundamental molecular vibration modes in the mid-infrared (400 to 4000 cm^{-1}). The absorbance/transmittance bands of each component in the mixture are proportional to the pure mineral spectrum (Matterson and Herron, 1993; Njoya *et al.,* 2006). This is known as Beer's Law, expressed as follows:

$$A = \sum_{i=1}^{n} \varepsilon_i 1 \, c_i \qquad (5)$$

Where *A* is the absorbance of a band, ε_i is the absorptivity of component i, 1 is the absorption path length (pellet thickness), and c_i is the concentration of component i.

The procedure used for FTIR spectrophotometry analysis was according to Ekosse (2005b). The infrared spectra for bulk kaolin and < 2 µm fraction were acquired using a Perkin Elmer system 2000 FTIR spectrophotometer at a resolution of 4 cm^{-1}. The < 2 µm kaolin fraction was obtained by centrifuge method (Tan, 1996). About 5 g of dried powdered samples were homogenized in spectrophotometric grade KBr in an agate mortar and pressed at 3 mm pellets with a hand press. In order not to distort the crystallinity of kaolinite in the samples, the mixing was set to 3 min allowing for minimal grinding as suggested by Tan (1996). Peaks were reported based on percentage transmittance to given wavelengths.

3.2.2.4 X-Ray fluorescence

The chemical composition of the bulk samples was determined by X-ray fluorescence spectrometry using a PANalytical Axios WDXRF spectrometer equipped with a 4 kW Rh tube in accordance with the method described by (Ekosse et al 2017). Milled samples with grain size of < 75 µm were heated at 1000 °C for 3 hours to oxidise Fe^{2+} and S and to determine the loss on ignition (LOI). One gram of heated sample and 9g of flux consisting of 34% $LiBO_2$ and 66% $Li_2B_4O_7$ were fused at 1050 °C to form stable glass disks. Each sample was analysed thrice and the mean recorded. For quality control, an in-house amphibolite reference material (12/76) was used to ensure accuracy of the data generated.

3.2.3 Technological analyses

Technological tests were carried out at the Council for Mineral Technology (MINTEK) South Africa, as part of the ceramic evaluation process. Clay samples were dried at 110 °C for 24 h and ground to a fine powder. The materials were mixed in a pan mixer with minimum quantity of water, suitable for extrusion in the Germatec Vacuum Extruder. Test briquettes were extruded into a column with cross section measuring 47 mm x 25 mm x 150 mm.

The briquettes were air dried for 5 days, followed by drying in a ventilated oven at 110 °C for 24 h until two successive weighing's at intervals of 2 h showed an increment of loss not greater than 0.2 % of the previously determined weight of the specimen. After drying, the briquettes were cooled in a drying room maintained at a temperature of 24 ± 8 °C, with a relative humidity between 30 and 70 %. The specimens were stored free from

drafts, unstacked, with separate placement, for a period of at least 4 hours until the surface temperature was within 2.8 °C of the drying room temperature. Specimens noticeably warm to the touch, were not used for any tests (Yongue-Fouateu et al., 2016; Temga et al., 2019).

The specimens were stored in the drying room at the required temperature and humidity until they were tested. The briquettes were fired at 900 °C using an electrically powered laboratory furnace at a heating rate of 80 °C/h and cooling time of 2 h. The fired specimens were tested for WL, BD, WA, LS and FS. A total of five tests were performed per mechanical property and the mean result reported.

3.2.3.1 Weight loss

Weight loss (WL) was calculated between 105 °C (Md) and peak firing temperatures (Mf) using the following formula:

$$\mathrm{WL}\ (\%) = \left[\frac{\mathrm{Md}-\mathrm{Mf}}{\mathrm{Md}}\right] \times\ 100 \qquad (2)$$

3.2.3.2 Bulk density

Bulk density (BD) of a specimen was obtained as the ratio of the fired specimen mass (Mf) to the measured volume (V) of the specimen:

$$\mathrm{BD}\ (\mathrm{g/cm^3})\ = \mathrm{Mf/V}$$

3.2.3.3 Water absorption

Water absorption (WA) was measured by weighing the dried briquette (M1) and the wet (M2), after immersion in water for 24 h:

$$\text{WA}\ (\%) = \frac{\text{M2}-\text{M1}}{\text{M1}} \times 100 \quad (4)$$

3.2.3.4 Linear shrinkage

Fired linear shrinkage (LS) was determined across indentations made 100 mm apart by a digital vernier calliper on the test briquettes. The dried specimens were measured at the indentations to determine its longitudinal shrinkage to the nearest millimetre. The measured lengths were subtracted from the indentations measured 100 mm to obtain the shrinkage in millimetres:

$$\text{LS}\ (\%) = 100 - \text{fired length}\ (\text{mm}) \quad (5)$$

3.2.3.5 Flexural strength

Flexural strength (FS) of briquettes was evaluated using the three-point bending test method (Yongue-Fouateu et al., 2016) using a Kingtest Auto 200 Press Machine at a loading rate of 20 mm/min. The modulus of rupture values of each specimen was calculated and reported to the nearest 0.01 MPa as follows:

$$\text{FS}(\text{MPa}) = \frac{3\ \text{FL}}{2\text{b}d^2} \quad (6)$$

Where; F = maximum load, L = distance between the supports (mm), *b* = net width of the specimen at the plane of failure (mm) and,*d* = depth of the specimen at the plane of failure (mm).

CHAPTER FOUR: RESULTS

4.1 Physical characteristics of raw clay

The results for particle size distribution (PSD), colour and consistency of the raw clay are presented in Table 4.1. The PSD for D1 comprised predominantly of 20 – 2 µm fraction (52%), whereas sample D2 comprised predominantly of > 20 µm (45%) and 20 –2 µm fractions (41%). According to the Munsell soil classification system, D1 and D2 were described as reddish yellow and strong brown respectively. Based on the clay Atterberg limits, D1 and D2 recorded PI of 20 and 17, with CA values of 1.0 and 1.21 respectively.

Table 4.1 Physical properties of raw clay materials

Sample	PSD (mass%)			Hue/value/chroma	Colour	Atterberg Limits (mass%)			
	> 20 µm	20–2 µm	< 2 µm			LL	PL	PI	CA
D1	28	52	20	7.5YR/7/8	Reddish yellow	67	47	20	1.0
D2	45	41	14	7.5YR/5/8	Strong brown	58	41	17	1.21

4.2 Mineralogical characteristics of raw clay

The mineralogy characterization of the studied clays is expressed in terms of the identified mineral phases, functional groups, and thermal behaviour.

4.2.1 Mineral phase identification

The concentrations of the identified minerals are reported as major, minor and trace constituents. The characteristic mineral assemblage comprised; quartz + kaolinite ± mica + microcline + goethite + hematite + anatase + ilmenite. Quartz occurred as major

constituent in both samples, while kaolinite, Goethite and Anatase are present as minor constituents (Table 4.2). The XRD pattern of Duthuni kaolins was characterized by weak kaolinite peaks and the absence of the 110-kaolinite peak (Fig. 4.1).

Table 4.2: Bulk rock mineralogy of representative samples from Duthuni kaolin

Samples	K	Q	M	Mx	G	H	A	Ilm
D1	++	+++	–	+	++	+	++	+
D2	++	+++	–	++	++	++	+	+

(+++) Major, (++) minor, (+) trace, (–) not detected: k-kaolinite; Q-quartz; M-mica; Mx-microcline; G-goethite; H-hematite; A-anatase; IIm-illmenite.

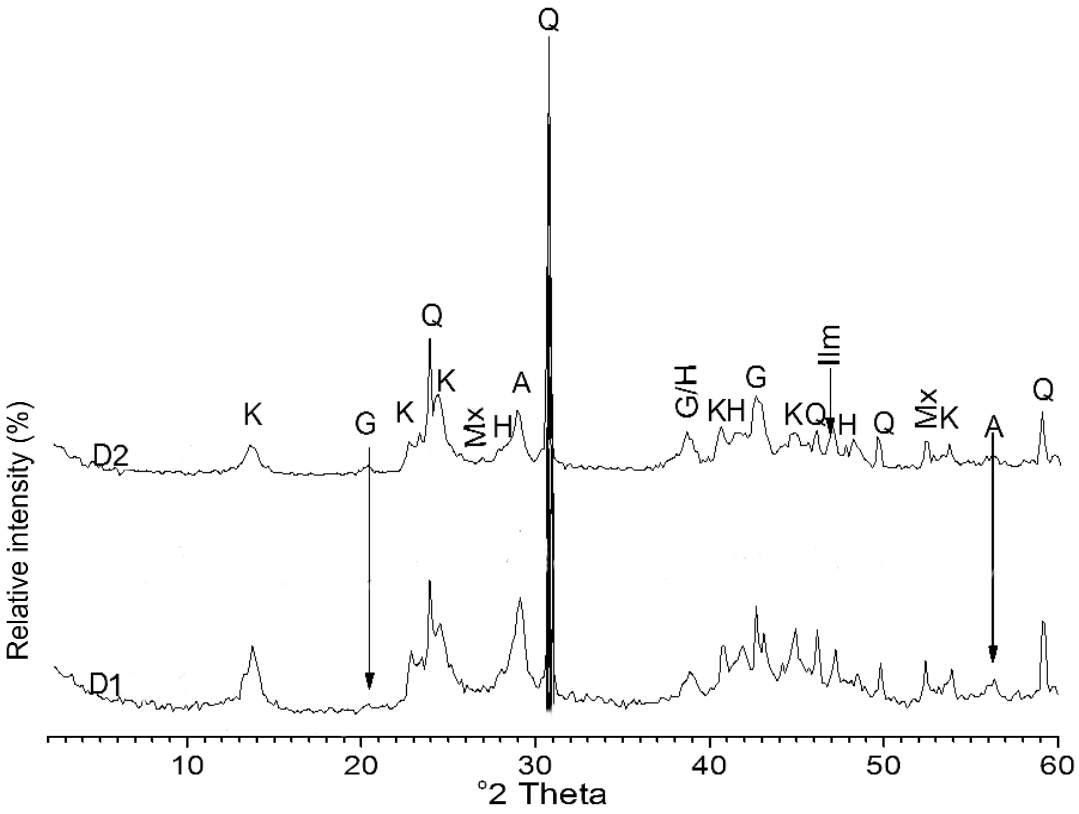

Figure 4.1 XRD patterns of raw clay materials

First and second order kaolinite peaks observed at 14.2º and 29.1º had maximum relative intensities of ≤ 19.42 % and ≤ 24.47 % respectively. The two most intense peaks observed at 24.18º (4.25 Å) and 31. 07º (3.33 Å) where assigned to quartz whereas the peak at 29.42º (3.52 Å) was assigned to anatase.

4.2.2 Functional group characteristics

The FTIR spectra of kaolin samples from Duthuni are presented in Table 4.3 and Figure 4.2. The samples exhibit two main OH stretching bands between 3619 and 3694 cm^{-1} and OH deformation within the region 907 cm^{-1} to 910 cm^{-1}. A low intensity peak at either 3650 cm^{-1} or 3651 cm^{-1} was observed in samples D2, whereas a doublet at 3650 cm^{-1} and 3651 cm^{-1} was observed in D1, accompanied by a weak shoulder at 3658 cm^{-1}. H-O-H stretching, and bending were also observed from 3227 cm^{-1} to 3391 cm^{-1} and between 1635 cm^{-1} and 1646 cm^{-1} respectively.

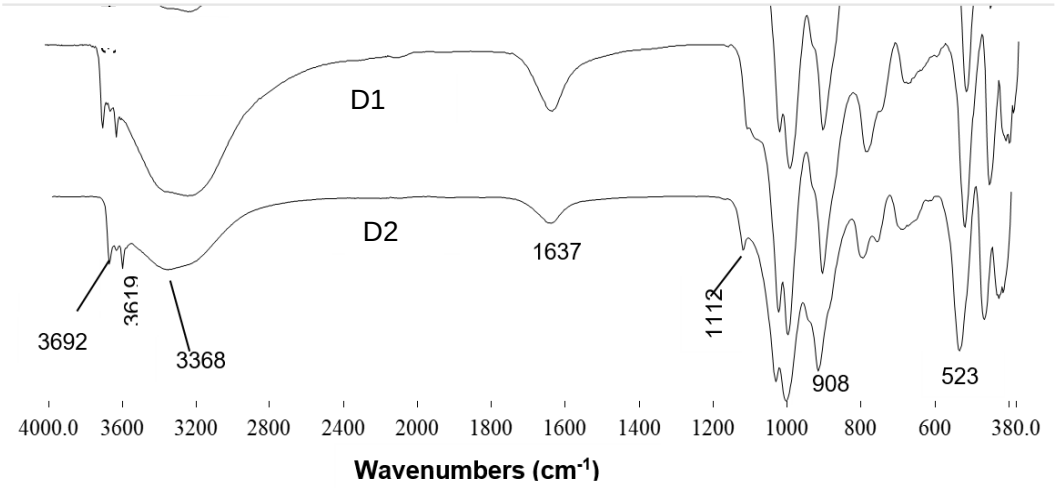

Figure 4.2 Infra-red spectra of representative bulk kaolin samples from Duthuni Kaolin.

Table 4.3 Assignments and infrared band positions of studied kaolin samples

Theoretical kaolinite	D1	D2	Assignment
3670 – 56	3692 3651	3690 3652	Al---O-H stretching of inner-surface hydroxyls
3645	3619	3619	Al---O-H stretching of inner hydroxyls
–	1411	1414	H-O-H stretching (absorbed water)
–	1653	1649	H-O-H bending; possibly smectite interference
1117 – 05	1111	1112	Si – O stretching
1035 – 30	1025	1024	Si – O stretching; muscovite interference
1019 – 05	999	996	Si – O quartz
918 – 09	908	908	OH deformation
800 – 784	– 793	– 789 748	OH deformation linked to Al^{3-},Mg^{2-}
700 – 686	686	679	Si – O quartz
542 – 35	524	522	* Fe-O, Fe_2O_3; Si-O-Al stretching
475 – 68	459	455	Si –O– Si bending
430	419 403 398	414 – –	Si – O deformation

4.2.3 Thermal behaviour

The measured DSC curves (Figures 4.3 and 4.4) showed the following endothermic effects; dehydration at low temperature interval from 85^{o}C to 90^{o}C, two dihydroxylation peaks from 295^{o}C to 300^{o}C and 530^{o}C to 535^{o}C. Melting, recrystallization and transformation of dehydrated mineral phases were observed as exothermic reactions at 955^{o}C for D1 and 945 ^{o}C for D2 respectively.

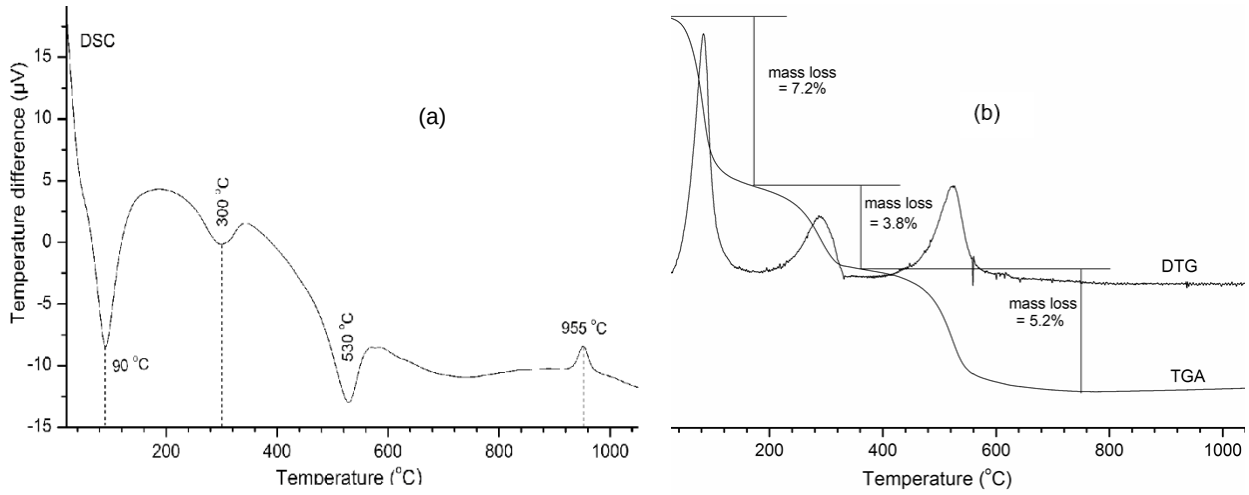

Figure 4.3 Thermal behaviour for sample D1. (a) DSC curve, (b) TGA/DTA Curve

Mass loses where observed between 20 ºC to 120 ºC (7.2% and 2%), 250 ºC to 320 ºC (3.8% and 1.3%) and 400 ºC to 600 ºC (5.2% and 6.2%) for D1 and D2 respectively.

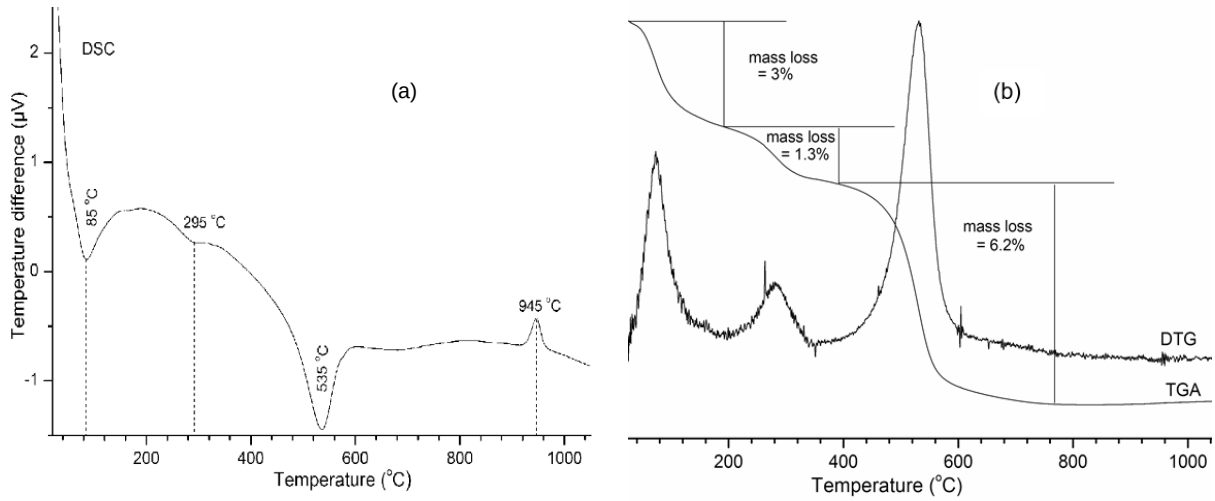

Figure 4.4 Thermal behaviour for sample D2. (a) DSC curve, (b) TGA/DTA Curve

4.3 Major oxide concentrations

Results from geochemical analysis are summarized on Table 4.4. The most abundant oxides in D1 and D2 were SiO_2, Al_2O_3, and Fe_2O_3. The concentration of SiO_2 was 38.49 – 45.45 wt %, Al_2O_3 (23.9 – 16.72 wt%) and Fe_2O_3 (23.49 – 21.29 wt%) in D1 and D2 respectively. The LOI was 9.94 wt% and 8.74 wt% for D1 and D2 respectively, while Si/Al ratio was 1.61 for D1 and 2.71 for D2. The alkali and alkali earth metals registered the lowest concentrations (ranging from 0.1 – 1.94 wt%).

Table 4.4 Chemical composition of the clay materials (wt%)

Sample	SiO_2	Al_2O_3	Fe_2O_3	CaO	K_2O	MgO	Na_2O	TiO_2	MnO	P_2O_5	LOI	Total	Si/Al
D1	38.49	23.9	23.49	0.11	0.1	0.16	0.01	2.91	0.27	0.14	9.94	99.55	1.61
D2	45.45	16.72	21.29	0.91	0.2	1.94	1.68	2.71	0.16	0.09	8.74	99.91	2.71

4.4 Technological Properties

A summary of the results for Weight Loss (WL), Bulk density (Bd), Water absorption (WA), Linear shrinkage (LS), and Flexural strength (FS) of the studied clays after heat treatment at four firing temperatures (800 ^oC, 900 ^oC, 1000 ^oC and 1100 ^oC) is presented on Table 4.5. Mean values of test results (n = 6) for the respective technological properties at all four firing temperatures are presented in Figures 4.5 to 4.9.

Weight loss in D1 ranged from 10.94% to 12.41% with increasing temperature from 800 to 1100 ^oC, whereas D2 reported values from 14.75% to 13.76% for same temperature range (Figure 4.5). A decrease in water absorption was observed in D2 after firing beyond 900 ^oC whereas an increase with firing temperature was observed in D1.

Table 4.5 Firing characteristics of raw clay materials

	Characteristics	800°C	900 °C	1000 °C	1100 °C
D1	Weight Loss (%)	10.94	11.89	11.50	12.41
	Bulk density (g/cm^3)	1.49	1.65	1.66	2.15
	Water absorption (%)	24.48	23.23	22.52	9.01
	Linear shrinkage (%)	10.20	11.72	12.44	18.59
	Flexural strength (MPa)	0.86	1	1.25	1.23
D2	Weight Loss (%)	14.74	16.96	16.08	13.76
	Bulk density (g/cm^3)	1.55	1.67	1.81	1.90
	Water absorption (%)	19.39	17.51	13.24	10.88
	Linear shrinkage (%)	8.06	9.27	11.26	11.84
	Flexural strength (MPa)	1.65	1.92	2.40	2.30

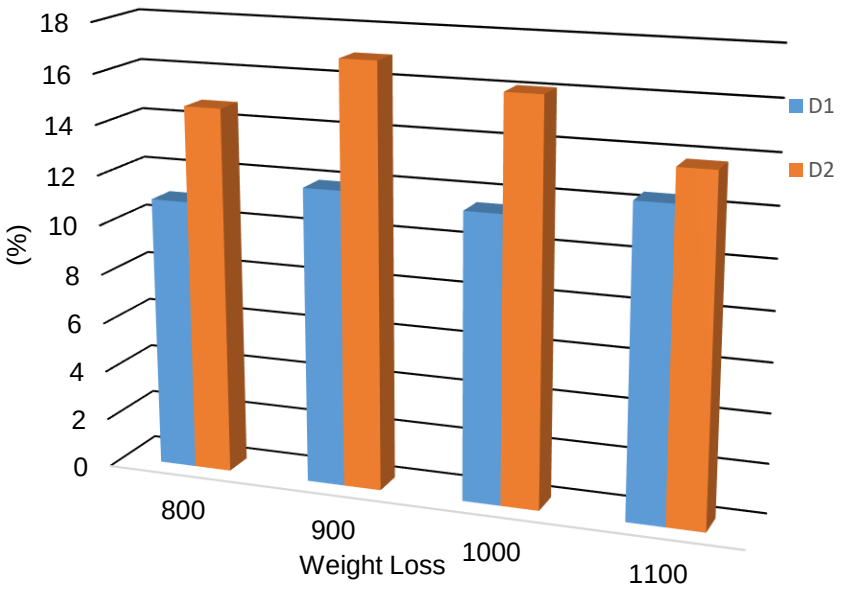

Figure 4.5 Variation of weight loss with temperature

Bulk density in D1 ranged from 1.49 g/cm^3 to 2.15 g/cm^3 with increasing temperature from 800 to 1100 ^{o}C, whereas D2 reported values from 1.55 g/cm^3 to 1.9 g/cm^3 for same temperature range (Figure 4.6). A general increase in bulk density with firing temperature was observed in both D1 and D2.

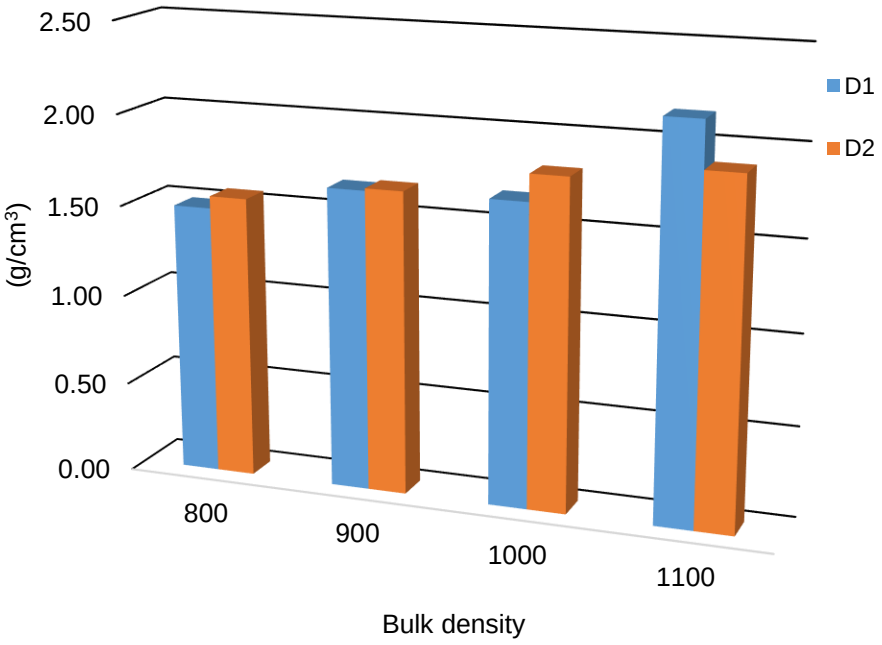

Figure 4.6 Variation of bulk density with temperature

Water absorption ranged from 24.48 % to 9.01% and 19.39% to 10.88% with increasing temperature from 800 to 1100 ^{o}C for D1 and D2 respectively (Figure 4.7). A general decrease in water absorption with firing temperature was observed in both D1 and D2. A steep decline was observed in both samples at 1100 ^{o}C.

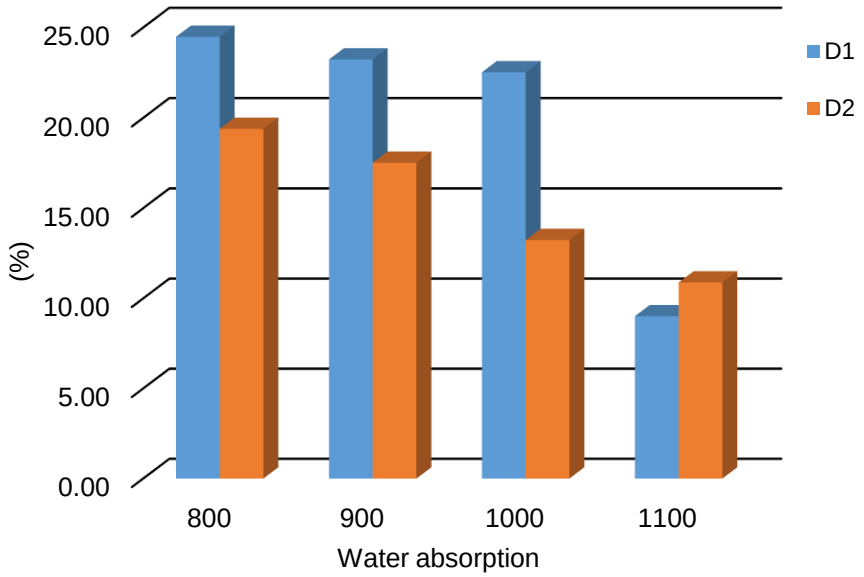

Figure 4.7 Variation of water absorption with temperature

Linear shrinkage in D1 ranged from 10.20% to 18.59% with increasing temperature from 800 to 1100 ^{o}C, while D2 reported values from 8.06% to 11.84% for same temperature range (Figure 4.8). A general increase in linear shrinkage with firing temperature was observed in both D1 and D2.

Flexural strength ranged from 0.86 MPa to 1.23 MPa and 1.65 MPa to 2.30 MPa with increasing temperature from 800 to 1100 ^{o}C for D1 and D2 respectively (Figure 4.8). A general increase in flexural strength with firing temperature was observed in both D1 and D2 up to 1000 ^{o}C. A steep decline was observed in both samples at 1100 ^{o}C.

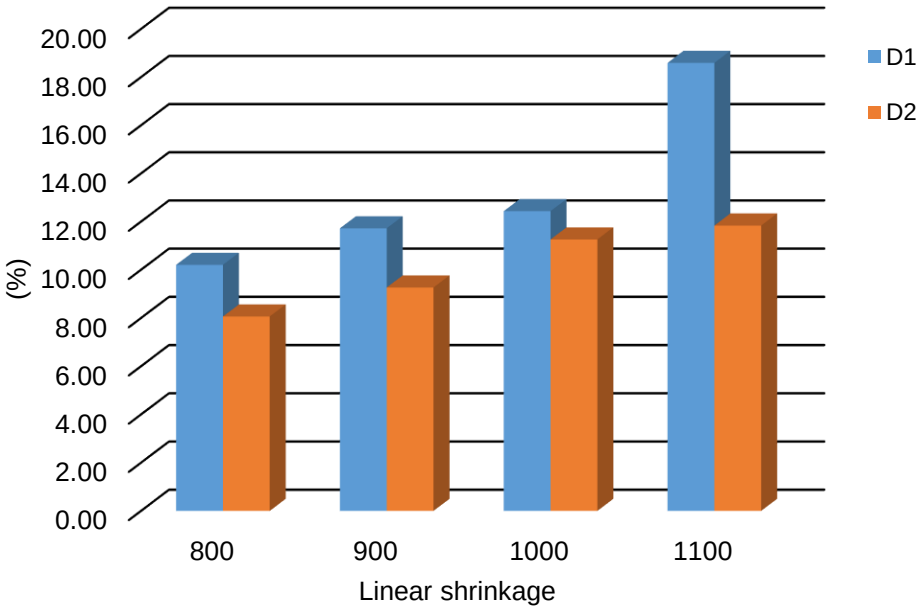

Figure 4.8 Variation of linear shrinkage with temperature

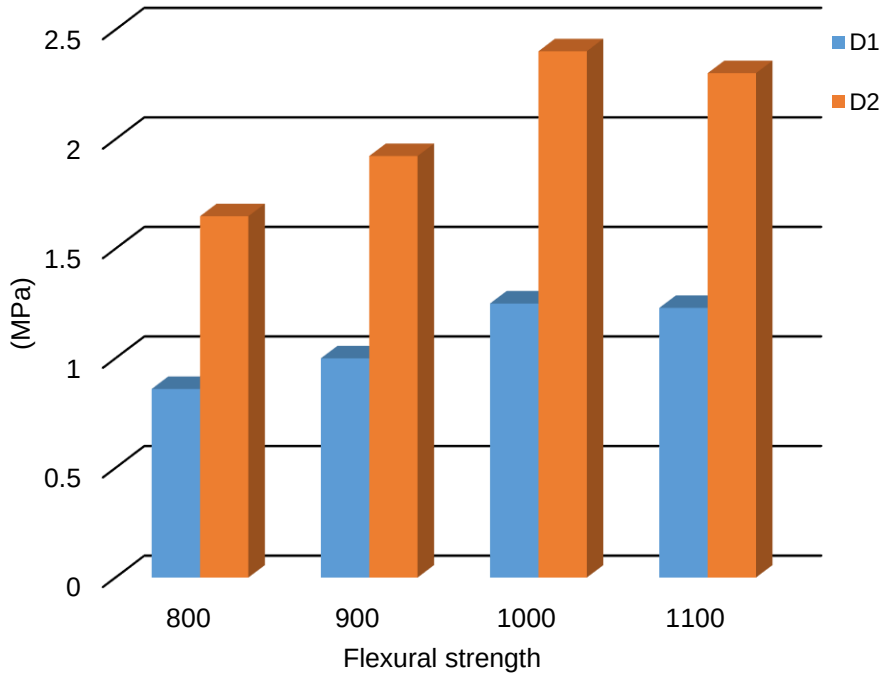

Figure 4.9 Variation of flexural strength with temperature

CHAPTER FIVE: DISCUSSIONS, CONCLUSIONS AND RECOMMENDATIONS

5.1 Effects of clay physical, mineralogical, and chemical property on ceramic suitability

5.1.1 Particle size distribution and clay texture

The PSD could be an indication of ceramic strength and applicability (Murray, 2000; Ekosse and Mulaba, 2008b). Clayey materials suitable for ceramics are classified as clayey silts and silty clay (Dondi et al., 1992; Strazzera et al., 1999; Ekosse and Mulaba, 2008a; Diko et al., 2011), including sandy clays, sandy silts, and loams (Semiz, 2017). Samples D1 and D2 were plotted on the sand – silt – clay ternary diagram (Fig. 5.1) proposed by Dondi et al. (1992) and Strazzera et al. (1999). Sample D1 was classified as silt loam whereas D2 was classified as loam.

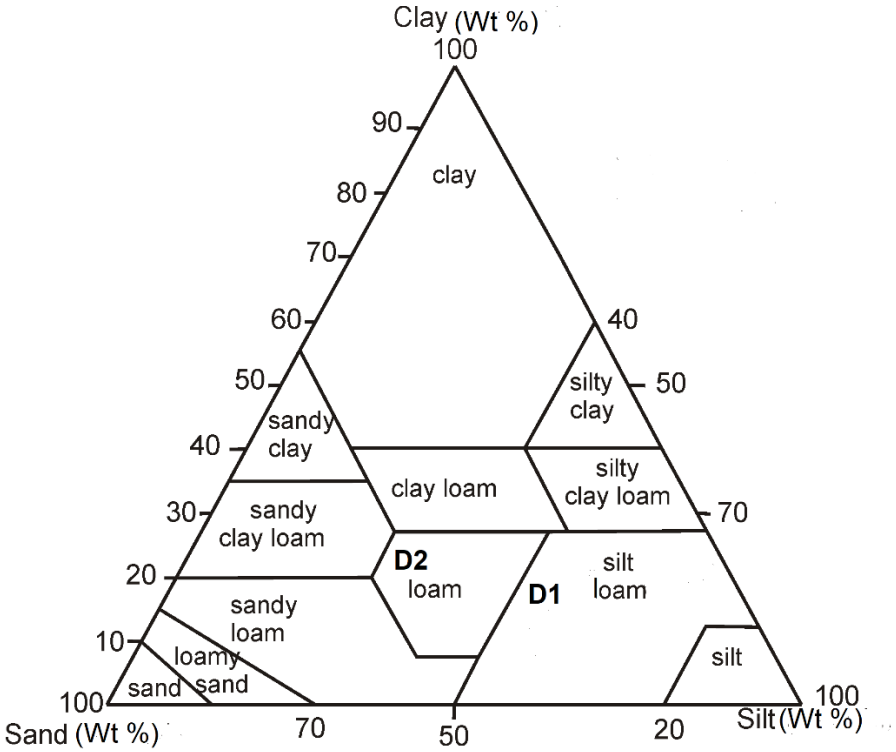

Figure 5.1 Clay texture (adapted from Dondi et al al., 2014?)

Although D1 and D2 do not satisfy the textural conditions proposed by Dondi et al (1992; 2014), and recommended by Diko et al (2011), the observed loam to silt loam textures are consistent with other raw clay materials from Ndop Plain – Cameroon (Yongue-Fouateu et al., 2016) as well as Amezmiz, Afyon, and Rio de Janeiro clays from Brazil (Semiz, 2017) and and Turkey (Celik, 2010; Semiz, 2017) which are being exploited for structural ceramics. The samples were functionally distributed using the grain size classification according to Winkler diagram (Fig. 5.2). Winklers diagram gives the allocation of clayey materials in their various fields of application; common bricks, vertically perforated bricks, roofing tiles masonry bricks and hollow products (Diko et al., 2011).

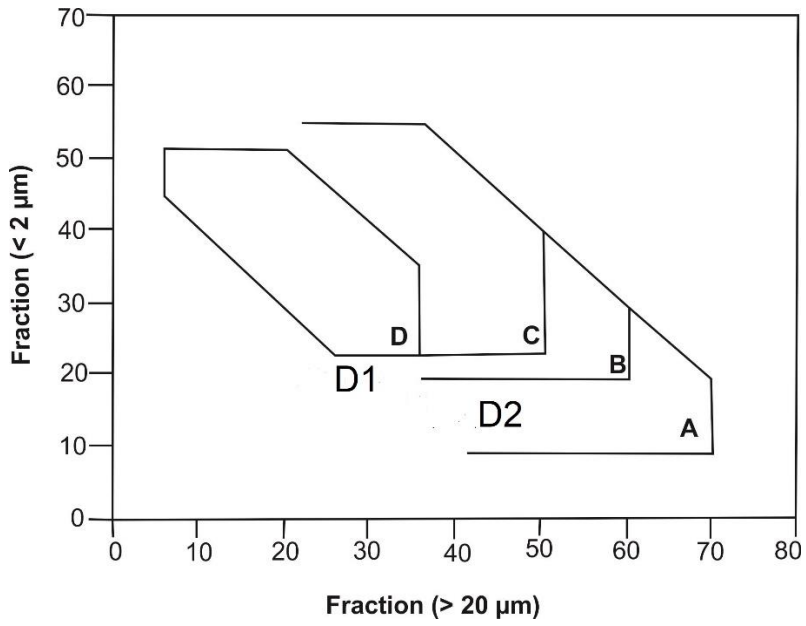

Figure 5.2 Grain size classification and applicability according to Winklers diagram: Fields are defined as: (A) common bricks, (B) vertically perforated bricks, (C) roofing tile and masonrybricks, and (D) hollow products (after Dondi et al., 1992, 2014)

Sample D1 plotted as an outlier for common bricks, vertically perforated bricks and hollow products, whereas D2 plotted within the common bricks field (Fig 5.2). The PSD and characteristic plots observed on the Winkler diagram are consistent with the current applications of the studied kaolins (manufacturing of face bricks). However with beneficiation in textural properties, the clay materials present potentials for exploitation beyond its predominant use as face bricks.

5.1.2 Raw clay colour

Colour of raw materials provides valuable insights into characteristics of the depositional environment and dominant pedogenic process. It is also an indicator of type and amount of iron oxides present and the resultant clay body colour after firing (Semiz, 2017). Based on hue/value/chroma of D1 and D2 (Table 4.1) designated colours are reddish yellow and strong brown respectively, with potential for forming dark-firing ceramics and light-firing ceramics (Dondi et al., 2014). The strong brown colour may be attributed to very poorly drained soils, high sand content or unoxidized iron compounds whereas the strong brown may do well drained soils or high iron oxidation compounds.

5.1.3 Clay consistency and mineralogy

The proportion of clay fraction in ceramic raw material is indicative of degree of plasticity and workability of the clay body (Diko et al., 2011; Diko and Ligege 2020). Although Koalin is a non-expansive clay mineral, its association with other phyllosilicates such as smectites and its fine particle size (< 2 µm) can increase the plasticity of raw kaolins (Murray, 2000). Clay consistency limits also serve as preliminary indicators of

mineralogical assemblages. This is based on the argument that clay activity is directly related to the type and amount of clay minerals (Diko and Ligege 2020).

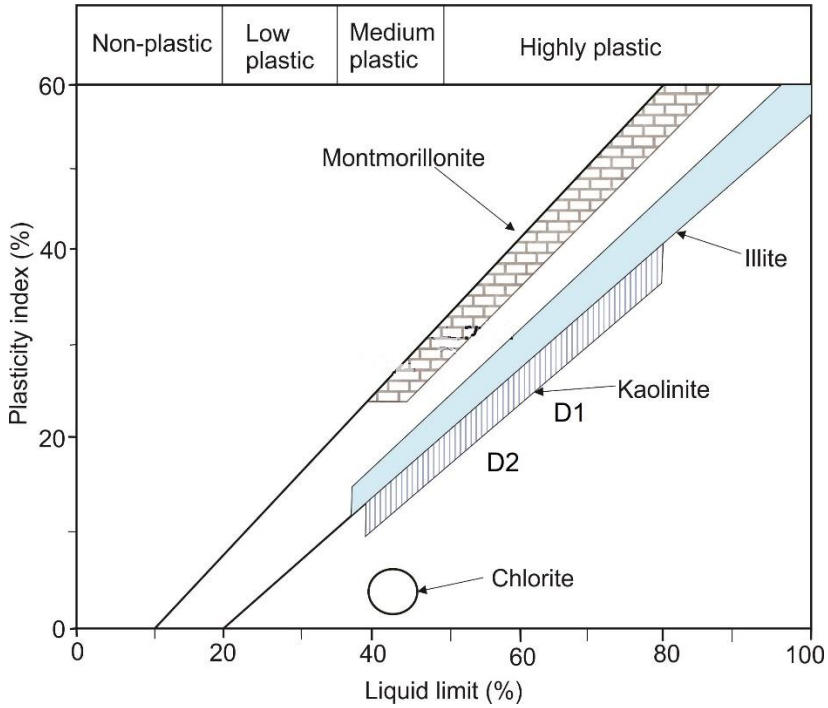

Figure 5.3 Consistency limits of raw clay materials according to Holtz and Kovacs (After Diko and Ligege, 2020)

The consistency limits of D1 and D2 are plotted on the Holtz and Kovacs diagram (Fig 5.3) and the clay workability chart (Fig 5.4). The raw materials are of medium to high plasticity (PI = 20 and 17, for D1 and D2 respectively), with kaolinite as most likely clay mineral. Visual appraisal of the clay workability chart indicated that D1 and D2 plot within the high shrinkage field, with D1 displaying comparatively higher potential for shrinkage than D2 (Fig 5.4). The potential for high shrinkage suggests possible detrimental effects during clay body formulation (extrusion and molding) as well as firing phases of the ceramic manufacturing process.

Interpretations drawn from the Holtz and Kovacs diagram (Diko and Ligege, 2020) are consistent the South African standards (SANS, 2007) and corroborates the mineral phases identified by XRD. Kaolinite was the main clay mineral in both samples, occurring as minor constituent. The loam to silty texture of D2 and and D1 respectively are consistent with the predominance of quart phases revealed by the XRD and Si – O functional groups observed in the IR.

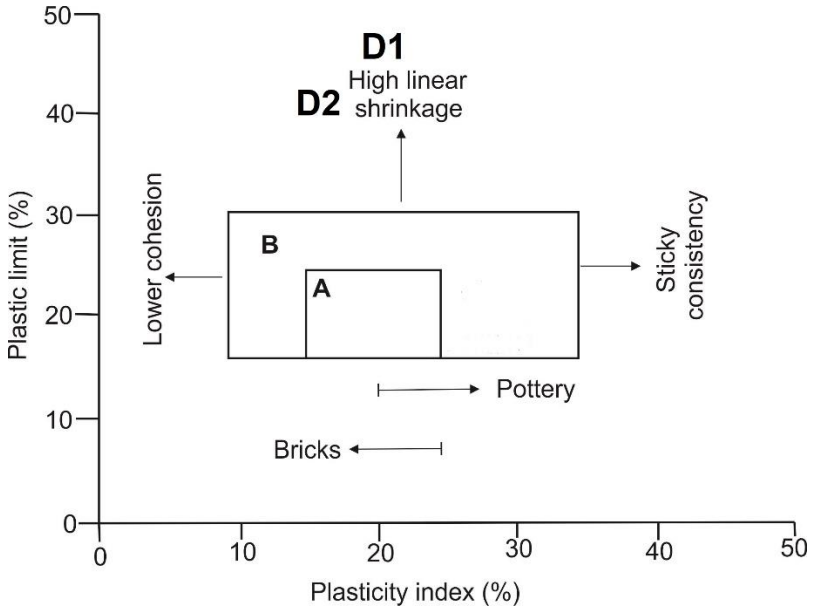

Figure 5.4 Clay workability chart

5.1.4 Chemical composition

The studied materials are siliceous (SiO_2: 38.5–45.5 wt%), aluminous (Al_2O_3: 23.9–16.7 wt%) and ferruginous (Fe_2O_3: 23.5–21.3 wt%), with the SiO_2/A Al_2O_3 ratios ranging from 1.61 to 2.71. The geochemistry of the clay samples also shows relatively high amounts of TiO_2 (2.91 – 2.71 wt% respectively for D1 and D2). According to Yongue-Fouateu et al

(2016), TiO_2 values ≥ 1.5 can be considered as high. Yongue-Fouateu et al (2016) further suggest that high Ti content is indicative of a mafic source rock. This observation is consistent with basaltic origin of the duthuni kaolin. The aluminous to ferruginous content, accompanied by depletion in alkali and alkali earth metals is also indicating on ongoing alteration. However, the presence of kaolinite as a minor constituent suggests that the kaolinization process is incomplete. The low kaolinite content and high iron oxide contents equally suggests kaolin impurity and colouring effect on the fired clays. Furthermore, appraisal of the ceramic suitability of D1 and D2 based on their geochemistry indicates suitability for red bodies (D2) and a close outlier for red bodies and porous tiles (Fig 5.5).

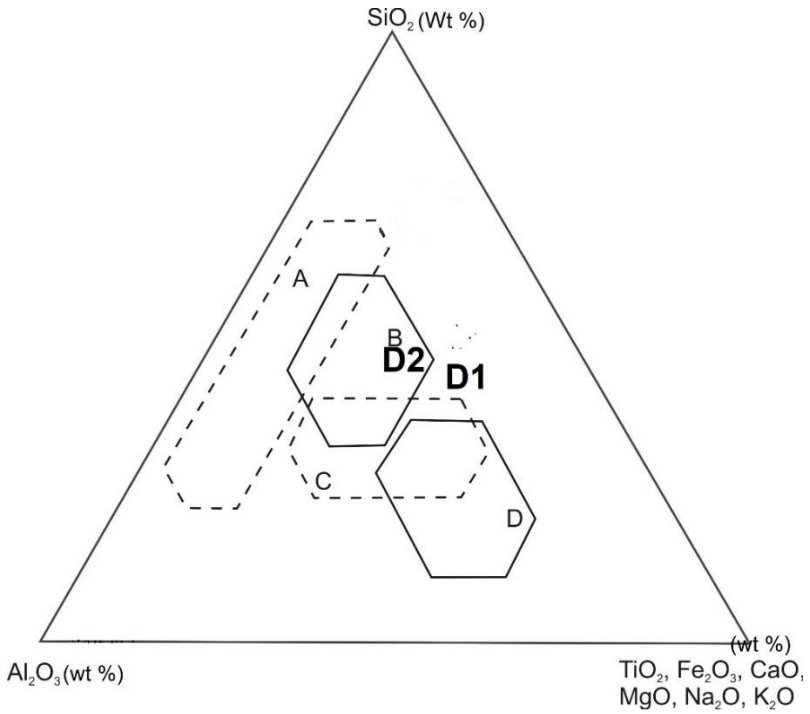

Figure 5.5 Clay chemical composition domains for preparing stoneware tiles (white (A) and red (B) bodies) and porous tiles (C and D).

5.2 Thermal evolution of ceramic raw materials

Kaolin group minerals are characterised by two major endothermic peaks and one exothermic peak (Ece et al., 2003). The exothermic peak corresponds to the destruction of the 1:1 kaolinite structure and is typically observed between 943^{o}C and 968 ^{o}C (Ece et al., 2003; Ekosse, 2008; Vaculikova et al., 2011). The dehydroxylation temperature of most kaolinites ranges from 498 ^{o}C to 605 ^{o}C, whereas the dehydroxylation of dickite and nacrite occurs at 680 ^{o}C (Ece et al., 2003; Ekosse, 2008). According to Ece et al. (2003) and Saviano et al. (2005) well-ordered kaolinites have broad endothermic peaks at ~ 590 ^{o}C while major weight losses during TG experiments occur between 400 and 600 ^{o}C.

The low temperature endothermic peak observed between 85 ^{o}C to 95 ^{o}C in representative samples Duthuni is indicative of loss of adsorbed water (Ece *et al.,* 2003; Ekosse, 2008; Vaculikova et al., 2011). A second endothermic peak observed between 295 ^{o}C and 300 ^{o}C is attributed to dehydroxylation reactions of goethite (α-FeO.OH) present in the above samples as indicated by XRD. This reaction led to the formation of hematite (equation 3) equally identified in the samples.

$$2\ \alpha\text{-FeO.OH} \rightarrow \alpha\text{-}Fe_2O_3 + H_2O \quad (3)$$

Goethite hematite

The DSC scans also portrayed samples having endothermic peaks between 500 ^{o}C to 560 ^{o}C, corresponding to dehydroxylation and transformation of kaolinite to metakaolinite as indicated below (equation 4) (Ekosse, 2008).

$$Al_2Si_2O_5(OH)_4 \rightarrow Al_2Si_2O_7 + H_2O \quad (4)$$

Kaolinite metakaolinite

Exothermic temperature peaks between 945 ^{o}C and 955 ^{o}C were attributed to the temperature range for mullite formation from metakaolinite as per equation 5 (Ece et al., 2003; Ekosse, 2008; Vaculikova et al., 2011).

$$\underset{\text{Metakaolinite}}{3Al_2Si_2O_7} \rightarrow \underset{\text{mullite}}{Al_6Si_2O_{13}} + 4SiO_2 \quad (5)$$

From DTG analyses, differential mass losses ranging from 10.5% to 16.2 % were attributed to dehydration reactions involving loss of adsorbed water and destruction of structural OH during kaolinite dehydroxylation. The lack of symmetry displayed by the DSC curves (Njoya et al., 2006), low kaolinite dehydroxylation temperatures (< 590 ^{o}C) associated with goethite dehydroxylation reactions observed in the studied kaolins, suggests low to moderate degrees of crystallinity (Ece et al., 2003; Saviano et al., 2005; Ekosse, 2008). According to Ekosse (2008), oxides and other associated non clay minerals may equally have influenced the reaction dynamics.

5.2 Technological properties

To appraise the technological performance of D1 and D2 after firing, their sintering properties were compared against globally adopted ceramic specifications for Weight loss (Teixeira et al., 2004), Linear shrinkage (Manukaji-John, 2013, Semiz, 2017), Flexural strength and Water absorption (Yongue-Fouateu et al., 2016, Souza et al., 2002; Teixeira et al., 2004).

5.2.1 Weight Loss

The highest percentage of weight loss (WL) was recorded at 1100 ^{o}C in D1(12.41%) and at 900 ^{o}C in D2 (16.96%). However, the WL for both samples at all firing temperatures was below the 14% threshold suggested by Teixeira et al. (2004). The comparatively high WL at 900 ^{o}C may be attributed to exothermic reactions involving mullite formation from metakaolinite (Ece et al., 2003; Ekosse, 2008; Vaculikova et al., 2011).

5.2.2 Bulk density

The bulk density (Bd) increased with firing temperature in both samples. The maximum Bd at 1100 ^{o}C may be associated with formation of a substantial glassy phase (Yongue-Fouateu et al, 2016). According to Ngun et al. (2011) the formation of a silicate liquid phase at 1100 ^{o}C also contributes towards increased densification and weight loss.

5.2.3 Linear shrinkage

Linear shrinkage gives an indication of the efficiency of firing and the internationally accepted value is 7–10% for aluminum-silicates, kaolin, and fired clays (Manukaji-John, 2013). Conversely, Yongue-Fouateu et al (2016) proposed values for LS (2 % – 10 %) as acceptable range for structural ceramics. The LS in D1 ranged from 10.2 % to 18.59% from 800 ^{o}C to 1100 ^{o}C. A corresponding increase in LS was also observed in D2 (8.06 % to 11.8%). Sample D1 did not meet the LS specifications of prescribed by Manukaji John (2013), Semiz (2017) and Yongue-Fouateu et al (2016). On the other hand, D2 satisfied the LS specifications at 800 and 900 ^{o}C. At higher firing temperatures the amount of fired shrinkage exceeded the acceptable values. The high LS is probably due to a more significant liquid phase formation. According to Ngun et al. (2011), the occurrence of liquid

surface tension during liquid phase formation helps to bring particles close together thereby reducing porosity and increasing LS.

5.2.4 Flexural strength

Ceramic specifications based on flexural strength (FS) are presented on Table 5.1. According to Yongue-Fouateu et al (2016) FS ranging from 1.2 – 11.8 MPa have frequently been used as quality and process control parameters in the development and manufacturing stages to produce structural ceramics. Souza et al. (2002) and Teixeira et al. (2004) also proposed FS classification criteria for various ceramic pieces The ceramic potential of D1 and D2 were appraised against the FS specifications (Table 5.1).

Table 5.1 Ceramic specifications based on flexural strength

	Ceramic piece		**Flexural strength (MPa)**			
			800ºC	**900 ºC**	**1000 ºC**	**1100 ºC**
		Indicated values*	0.86	1	1.25	1.23
D1	Not classified	< 1.96	√	√	√	√
	Massive bricks	≥ 1.96	X	X	X	X
	Ceramic blocks	≥ 5.39	X	X	X	X
	Roof tiles	≥ 6.37	X	X	X	X
		Indicated values	1.65	1.92	2.40	2.30
D2	Not classified	< 1.96	√	√	√	√
	Massive bricks	≥ 1.96	X	X	√	√
	Ceramic blocks	≥ 5.39	X	X	X	X
	Roof tiles	≥ 6.37	X	X	X	X

* Values after Souza et al. (2002), Teixeira et al. (2004).

The FS of D1 increased steadily up to 1000 ºC and then experienced a slight decline at 1100 ºC. The FS values for D1 ranged from 0.86 to 1.25 MPa, with acceptable strength

attained at 1000 ^{o}C and 1100 ^{o}C with reference to the Yongue-Fouateu et al (2016). However, in terms of the Souza et al. (2002) and Teixeira et al. (2004) specifications, D1 did not meet the requirements for massive brick, roof tile and ceramic block (Table 5.1). The FS of D2 showed a similar increasing trend and slight decline at 1100 ^{o}C. The FS values were however higher than those recorded for D1 (1.65 to 2.40 MPa) and satisfied the specifications prescribed by Yongue-Fouateu et al (2016) for all firing temperatures. In terms of the Teixeira et al. (2004) specifications, D2 satisfied the conditions for massive bricks at 1000 ^{o}C and 1100 ^{o}C (Table 5.1).

5.2.5 Water absorption

Water absorption (WA) of raw ceramic materials is critical for its exploitation and defines the quality of finished product. Low to medium water absorption capacity has an inverse relationship with the durability and strength of ceramic ware (Semiz 2017). Water absorption > 25% is suitable for the manufacture of refractories. If WA is < 25% but > 20%, the clay is indicated to produce baked bricks, and if WA is < 20%, the clay is suitable for the manufacture of the tiles (Souza et al., 2002; and Teixeira et al.,2004).

Table 5.2. Ceramic specifications based on water absorption

			Water absorption (%)			
			800°C	900 °C	1000 °C	1100 °C
	Ceramic piece	Indicated values*	24.48	23.23	22.52	9.01
D1	Massive bricks	≤ 25	√	√	√	√
	Ceramic blocks	≤ 25	√	√	√	√
	Roof tiles	≤ 20	X	X	X	√
			19.39	17.51	13.24	10.88
D2	Massive bricks	≤ 25	√	√	√	√
	Ceramic blocks	≤ 25	√	√	√	√
	Roof tiles	≤ 20	√	√	√	√

* Values after Souza et al. (2002), Teixeira et al. (2004).

The WA for D1 showed a decrease with firing temperature, ranging from 24.48 % at 800 °C to 9.01% at 1100 °C. A similar trend was observed for D2 (19.39 % to 10.88 %) from 800 °C to 1100 °C respectively. Based on the WA specifications proposed by Souza et al. (2002) and Teixeira et al. (2004) D1 meets the requirements for production of massive bricks and ceramic blocks at all temperatures while D2 satisfies the conditions for massive bricks, ceramic blocks and roof tiles (Table 5.2.)

5.4 Ceramic Suitability

The mineralogical constituents of ceramic pastes range from clay minerals as plastic and binder components to siliceous sand as skeletal components and finally feldspars and/or fine carbonates as fluxing agents (El Boudour El Idrissi et al., 2018). During the firing process, the main constituents of raw clay undergo phase transformations through decomposition to produce neomineralization like metakaolinite and spinel at about 900 °C (Aramide, 2012) and mullite, cristobalite and wollastonite at higher temperatures (El Boudour El Idrissi et al., 2018). The higher the temperature, the more likely the

predominance of viscous flow sintering and densification of the fired body (Diko et al 2011). However, similar effects may be achieved at comparatively lower temperatures if the raw clay has the right mix of binders, skeletal components and fluxing agents. The predominance of silt-size fractions (comprising quartz and feldspar grains) in the studied clays samples suggest that PSD may contribute positively towards clay body skeleton, glass formation and lowering of vitrification temperature (Diko et al., 2011; Semiz, 2017).

The studied clays show moderate potentials for exploitation based on their inherent characteristics. This limits the exploitation to predominantly face bricks. To increase the value of Duthuni kaolin, there is need for beneficiation. Mixing of D1 and D2 may compensate for weakness observed in the clay texture, clay consistency, thermal behaviour and technological properties. Alternatively low plastic, high purity kaolin can be sourced, however this approach may be cost ineffective.

5.5 Conclusions

This study investigated the ceramic suitability of two representative kaolin samples from Duthuni area, subjected to four firing temperatures (800 ^{o}C, 900 ^{o}C, 1000 ^{o}C and 1100 ^{o}C). The objectives were to ascertain the effects of the raw clay physical, mineralogical, chemical characteristics on its ceramic potential, elucidate on the thermal evolution and associated mineral phase transformations, and to technologically characterize the raw clays. The following conclusions can be drawn.

- The raw materials are textural described as loam and silty loam with a high potential for shrinkage, suggests possible detrimental effects during clay body

formulation (extrusion and molding) as well as firing phases of the ceramic manufacturing process.

- Evaluation of ceramic specifications based on Winkler's diagram, clay workability chart, SANS 227 and various compositional ternary diagrams reveals poor to moderate extrusion properties and limited ceramics applicability.
- Mechanically, the raw clays show acceptable WL Bd WA LS but generally low FS.
- These results infer partial/incomplete kaolinisation processes and significant amount of impurities (e.g. quartz and iron oxide contamination).
- Free quartz serves as non-plastic filler, reducing the strength, plasticity and drying contraction.
- Iron oxide influences fired colour of the finished product. This also influences market value of the clay brick (cream to whitish comparatively more expensive than red).

Based on the current findings, the following recommendations are advanced for further investigation:

- Detailed mineralogical appraisal of fired bricks to ascertain mullite formation process.
- An addition of fluxing agent should be considered to improve the sintering of these clays.
- Blending with less plastic material is recommended to improve on extrusion and moulding property of raw clay material.

REFERENCES

Aduba, B.O., Nyongesa, W.F., Obado, G., 1999. Improving the green and fracture strength of a kaolinite ceramic using some vegetable syrup. Journal of Material Science Letters 18 (20), 1653-1655

Aly, M.H., 2002. Utilization of some Egyptian raw material in the production of porcelainised stoneware tile. Tile and Brick International 18 (2), 92-95

Aramide, M., 2012. Effect of Firing Temperature on Mechanical Properties of Fired Masonry Bricks Produced from Ipetumodu Clay. Leonardo Journal of Sciences, 21; 70-80.

ASTM, 1999a. Flexural Properties of Ceramic Whiteware Materials, C 674-88. American Society for Testing and Materials, West Conshocken, PA.

ASTM, 1999a. Water Absorption, Bulk Density, Apparent Porosity, and Apparent Specific Gravity of Fired Whiteware Products, C 373-88. American Society for Testing and Materials, West Conshocken, PA.

Baccour, H., M., Jamoussi, F., Mhiri, T., 2009. Influence of firing temperature on the ceramic properties of Triassic clays from Tunisia. Journal of Material Processing and Technology. 209, 2812-2817.

Baioumy, H.M., Ismael, I.S., 2014. Composition, origin and industrial suitability of the Aswan ball clays, Egypt. Applied Clay Science 102, 202–212. https://doi.org/10.1016/j.clay.2014.09.041.

Barker O. B., 1983. A Proposed Geotectonic Mode of Soutpansberg Group within the Limpopo Mobile Belt. Geological Society of South Africa.Pp181-190

Bittelli, M., G. S. Campbell, and Flury, M., 1999. Characterization of Particle-Size Distribution in Soils with a Fragmentation Model. Journal of Soil Science Society of America 63:782-788.

Blatt, H., Middleton, G., and Murray, R., 1980. Origin of sedimentary rocks .2nd ed.): Englewood Cliffs, N.J., Prentice-Hall, p. 766.

Bohlender F., Van Reenen D.D. and Barton J.M., 1992. Evidence for Metamorphic and Igneous Charnockites in the Southern Marginal Zone of the Limpopo Belt, South Africa. Precambrian Research. 55: 429-449.

Boulingui, J.E., Nkoumbou, C., Njoya, D., Thomas, F., Yvon, J., 2015. Characterization of clays from Mezafe and Mengono (Ne-Libreville, Gabon) for potential uses in fired products. Applied Clay Science 115, 132–144. https://doi.org/10.1016/j.clay.2015.07.029.

Boussen, S., Sghaier, D., Chaabani, F., Jamoussi, B., Bennour, A., 2016. Characteristics and industrial application of the Lower Cretaceous clay deposits (Bouhedma Formation), Southeast Tunisia: potential use for the manufacturing of ceramic tiles and bricks. Applied Clay Science 123, 210–221. https://doi.org/10.1016/j.clay.2016.01.027.

Brandl G., 1999. Soutpansberg Group. Catalogue of South African Lithostratigraphic Units, SA Committee for Stratigraphy, Council for Geoscience, pp.6-41.

Brindley, G. W., Brown, G., 1980. Crystal Structure of clay Minerals and their X-ray Identification. Mineralogical Society, London.

Burst, J.F., 1991. The application of clay minerals in ceramics. Applied Clay Science 5,421-443. Cambodia, 1993. Economic and social commission for Asia and the Pacific. Atlas of Mineral Research of the ESCAP Region, vol. 10. United Nations Publication

Carter M.R. and Gregorich E.G., 2008. Soil sampling and methods of analysis. Canadian society of soil science. CRC Press. P 731.

Cases, J.M., Lietard, O., Yvon, J.F., 1982. Etude de proprieties crystallochimiques, morphologiques, superficielles de kaolinites desordonness. Bulletin de Mineralogie 105 439-455.

Celik, H., 2010. Technological characterization and industrial application of two Turkish clays for the ceramic industry. Applied Clay Science 50, 245–254. https://doi.org/10.1016/j.clay.2010.08.005.

Chandrasekaran, S., Venkataraman Gupta, E.V., Chauhan, M.M., Baily, G.V., Chaudhuri, K., 1990. Serodiagnosis of pulmonary tuberculosis by kaolin agglunination test. Indian Journal of Tuberculosis 37, 11-15.

Christidis, G., 1998. Physical and chemical properties of some bentonite deposits of the Kimolos Island, Greece. Applied Clay Science 13, 79-98.

Christidis, G., Scott, P., 1997. The origin and control of colour of white bentonites from Aegean is land of Milos and Kimolos, Greece. Mineralium Deposita 32. 271-279.

Department of Mineral and Energy, 2005. The kaolin industry in the Republic of South Africa. Annual Report R47/2005, p. 57. http://www.dme.gov.za Accessed, 13/09/2008.

Diko ML and Ligege R., 2020. Composition and technological properties of clays for structural ceramics in Limpopo (South Africa). Minerals, 10, 700; doi:10.3390/min10080700.

Diko, M.L., Banyini, S.C. Monareng, B.F., 2014. Landslide susceptibility on selected slopes in Dzanani, Limpopo Province, South Africa', Jàmbá: Journal of Disaster Risk Studies 6(1), Art. #101, 7 pages. http://dx.doi.org/10.4102/jamba.v6i1.101

Diko, M.L., Ekosse, G.E., Ayonghe, S.N., Ntasin, E.B., 2011. Physical characterization of clayey materials from tertiary volcanic cones in Limbe (Cameroon) for ceramic applications. Applied Clay Science 51, 380–384. https://doi.org/10.1016/j.clay.2010.11.034.

Dondi, M., Fabbri, B., Laviano, R., 1992. Characteristics of the clays utilized in the brick industry in Apulia and Basilicata (Southern Italy). Mineral Petrologica Acta 35, 181–191.

Dondi, M., Raimondo, M., Zanelli, C., 2014. Clays and bodies for ceramic tiles: reappraisal and technological classification. Applied Clay Science 96, 91–100. https://doi.org/10.1016/j.clay.2014.01.013.

Du Toit M.C., Van Reenen D.D. and Roering C., 1983. Some aspects of the Geology, Structure and Metamorphism of the Southern Marginal Zone of the Limpopo Metamorphic Complex. In: Van Biljon W.J. and Legg J.H (Editor). The Limpopo Mobile Belt. Special Publication of the Geological Society of South Africa. 8: 121-142.

Ekosse, G.,1994: Clay a gateway into the future. Botswana Notes and Records 26, 139-149.

Ekosse G.E, Ngole-Jeme, V.M. and Diko ML., 2017. Environmental Geochemistry of Geophagic Materials from Free State Province in South Africa Open Geoscience 9:114–125DOI 10.1515/geo-2017-0009

Ekosse, G., 1998. The kaolin industry in Africa: genesis, industrial applications, investment prospects and futures economic trends. Industrial Minerals 372, 77.

Ekosse, G., 2000. The Makoro kaolin deposit, southeastern Botswana: its genesis and possible industrial applications. Applied Clay Science 20, 137-152.

Ekosse, G., 2001a. Provenance of the Kgwakgwe kaolin deposit, southeastern Botswana and its possible utilization. Applied Clay Science 20, 137-152.

Ekosse, G., 2001b. The kaolin industry in Botswana. Building and Construction Botswana 1, 27-36.

Ekosse, G., 2005. Fourier transforms infrared spetrophotometry and X-ray powder diffractometry as complementary technique in characterizing clay size fraction

of kaolin. Journal of Applied Science and Environmental Management 9 (2), 43-48.

Ekosse, G., 2010. Kaolin deposits and occurrences in Africa: Geology, Mineralogy and utilization. Journal of Applied Clay Science 50, 212-236.

Ekosse, G.E., Mulaba A., 2008a. Granulometric Evaluation of Continental Bentonites and Kaolin for Ceramic Applications. Journal of Applied Sciences. 8 (6), 1021-1027.

Ekosse, G., Mulaba-Bafibiandi, A.F., 2006. Diagnostic evaluation of bentonitic and kaolinitic clayey materials for possible ceramic applications. Journal of the Cameroon Academy of Sciences 5 (2&3), 131-138.

Ekosse, G., Mulaba-Bafibiandi, A.F., Nkoma, S., 2007. Physico-chemistry of continental bentonites and kaolin for ceramic applications. African Journal of Science and Technology 8 (1), 107-115.

Ekosse, G.E., Mulaba, A., 2008b. Mineral thermochemistry of bentonite and kaolinite related to their possible application in the ceramic industry. Journal of Applied Sciences. 8 (22), 4145 – 4151.

Ekosse, G., Mulaba-Bafubiandi, A.F., 2003. Kaolin occurrences in Botswana and possible uses as functional fillers. Proceedings of the 16th Industrial Minerals International Congress, Montreal, Canada. ISBN: 1 904333 079, PP. 68-80.

Ekosse, G., Nkoma, J.S., 2000. An investigation of the mineralogy, physic-chemistry and plasticity of the clayey material from the Makoro kaolin deposit, Botswana. Botswana Journal of Technology 9, 15-23.

Ekosse, G., Shemang, E., 2002. Petrography, mineralogy, chemistry and possible industrial applications of some selected kaolin deposits from Bauchi, Northerastern Nigeria and Kgwakgwe, Southeastern Botswana. In: Ngowi, A.B., Feldman, C., Matshediso, B., Mathiba, J., Segawa, S.J. (Eds.), proceeding of the 1st Botswana International Conference on Mining. Challenges Facing the Mineral Industry in Developing Countries 20-22 November 2002, pp. 107-116.

Ekosse, G., Van der Heever, D.J., de Jager, L., Totolo, O., 2003. Environmental mineralogy of soils around Selebi Phikwe nickel-copper plant, Botswana International Journal of Environmental Studies. 60, 251-262.

Ekosse, G., Vink, B., 2001. The geology and mineralogy of the Kgwakgwe basin lower Transvaal super group, Kanye area Botswana. Botswana Journal Earth Sci 5, 11-20.

El Boudour El Idrissi H, L Daoudi, M El Ouahabi, F Collin, Fagel, N., 2018. The influence of clay composition and lithology on the industrial potential of earthenware. Construction and Building Materials 172, 650–659.

El Halim M, L Daoudi, M. El Ouahabi, J. Amakrane , Fagel, N., 2018.Mineralogy and firing characteristics of clayey materials used for ceramic purposes from Sale region (Morocco). Journal of Materials and Environmental Science, 9 (8), pp. 2263-2273

El Ouahabi, M., Daoudi, L., Fagel, N., 2014. Mineralogical and geotechnical characterization of clays from northern Morocco for their potential use in the

ceramic industry. Clay Minerals 49, 35–51. https://doi.org/10.1180/claymin.2014.049.1.04.

El-Dine, W.N., Sroor, A., El-Bahi, S.M., Ahmed, F., 2004. Radioactivity in local and imported kaolin types used in Egypt. Applied Radiation and Isotope 60 (1), 105-109.

Fadil-Djenabou, Ndjigui, J, Bukalo, N., Ekosse GE., 2023. Effect of the incorporation of Neem (*Azadirachta indica*) wood ash in Kodeck ceramic materials for the manufacture of fired bricks (Far-North Cameroon). Heliyon 9 (2023) e14335

Fiori, C., Fabbri, B., Donati, F., Venturi, I., 1989. Mineralogical composition of the clay bodies used in the Italian tile industry. Applied Clay Science. 4, 461–473.

Garzon, E., Sanchez-soto, P.J., Romero, E., 2010. Physical and geothnical properties of clay phyllites. Applied Clay Science 48, 307-318.

González, I., Romero-Baena, A., Galán, E., Miras, A., Castilla-Alcántara, J.C., Campos, P., 2018. Ceramic materials from Cuatrovitasarchaelogical site (Spain). A mineralogical and chemical study for determining the provenance and the firing temperature. Applied Clay Science 166, 38–48. https://doi.org/10.1016/j.clay.2018.09.003.

Harry O. Brady, Nyle C., 1960. The Nature and Property of Soils - A College Text of Edaphology (6th ed.), New York: Macmillan Publishers, New York, NY, p. 50.

Hashimu H, Park, SE, Choi, B, An, Y, Jeongin J., 2014. Influence of Firing Temperature on Physical Properties of Same Clay and Pugu Kaolin for Ceramic Tiles

Application. International Journal Material Science Application. 3(5), pp. 143-146. doi: 10.11648/j.ijmsa.20140305.12

Hillel, D. and Hillel, D., 2004. Introduction to Soil Physics. USA: Academic Press.

Hinckley, D.N., 1963. Variability in crystallinity values among the kaolin deposits of the coastal plains of Georgia and South Carolina. Clays and Clay Minerals 11, 229-235.

Hope, C.A., 2001. Egyptian Pottery. Shire Publications Ltd, Comwell House, UK.

Hradil, D., Hradilová, J., Holcová, K., Bezdičk, P., 2018. The use of pottery clay for canvas priming in Italian Baroque – an example of technology transfer. Applied Clay Science. 165,135–147. https://doi.org/10.1016/j.clay.2018.08.011.

ICDD, 2001. Mineral Powder Diffraction File Data Book SETS 1-50. International Centre for Diffraction Data, Newtown Square, PA, USA. 941 pages.

Jenkins, R.,1999. X-ray fluorescence spectrometry: second edition. New York: Wiley-Interscience.

Joseph-Marie, Raunel, L Timothée, S, Mozalin, FP., 2019 Characterization and technological properties of two clay soils in Republic of Congo. Res. J. Material Sci.Vol. 7(1), 1-10.

Konta, J., 1995. Clay and man: clay raw materials in the service of man. Applied Clay Science 10, 275-335.

Lachen, D., Elboudour, E.i H., Saadi, L., Albizane, A., Bennazha, J., Waqif, M., Elouahabi, M., Fagel, N., 2014. Characteristics and ceramic properties of clayey materials

from Amezmiz region (Western High Atlas, Morocco). Applied Clay Science 102, 139–147. https://doi.org/10.1016/j.clay.2014.09.029.

Lal R. And Shukla M.J., 2004. Principles of Soil Physics. New York: Marcel Dekker, P 86-139,214-233.

Langdon, J., Robertshaw, P., 1985. Petrographic and physico-chemical studies of early pottery from South-Western Kenya. Archaeological Research in Africa 20 (1), 1-28.

LCPC, 1987. Limites d' Atterberg, limite de liquidite, limite de plasticite. Laboratoire Central des Ponts et Chaussees No. 19.

Lee, V.G., Yeh, T.H., 2008. Sintering effects on the development of mechanical properties of fired clay ceramics. Mat. Sci. Eng. A 485, 5-13.

Manukaji John, U., 2013. Chemical and mechanical characterization of clay samples from Kaduna State Nigeria. Int. J. Eng. Invent. 2–7 (20–26).

Mapuna, ECN., Aye, BA., Ntouala, R, Ndjigu PD., Bilong P., 2023. Mineralogical, geochemical, and physicomechanical features of the Mbalmayo lateritic clays (Southern Cameroon) for potential use as raw materials in the making of fired bricks. Arabian Journal of Geosciences 16:671

Martín-Márquez, J, J. Ma. Rincón and Romero, M., 2008. Effect of firing temperature on sintering of porcelain stoneware tiles, Ceramics Internacional, 34,1867-1873; doi:10.1016/j.ceramint.2007.06.006

Massachusetts institute of Technology, 2004. Kenya Water and Sanitation Program Project Proposal. Massachusetts Institute of Technology Aqua Social Journeys International, Massachusetts USA.

Michailidis, K., Tsirambides, A., 1986. The kaolin deposits of Leucogia, N. E. Greece. Clay Minerals 21, 417-426.

Mohmoudi, S., Srasra, E., Zargouni, F., 2008. The use of Tunisian Barremain clay in the traditional ceramics industry: optimization of ceramic properties. Applied Clay Science. 42, 125-129.

Moutou, J.M.,Foutou, P.M., Matini, L., Samba, V.B., Mpissi, Z.F.D. and Loubaki, R., 2018. Characterization and Evaluation of the Potential Uses of Mouyondzi Clay. Journal of Minerals and Materials Characterization and Engineering, 6, 119-138.

Murray, H.H., 1999. Applied clay mineralogy today and tomorrow. Clay Minerals. 34, 39-49.

Murray, H.H., 2000.Traditional and new applications for kaolin, smectite, palygorskite: a general overview, Applied Clay Science. 17, 207–221.

Murray, H.H.,1994. Common clay. Chapter in Industrial Minerals and Rocks, 6th Edition. Carr, D.D., ed. Society for Mining, Metallurgy and Exploration, Littleton, CO, pp. 247–248.

Murray, H.H., 2007. Applied Clay Mineralogy: Occurrences, Processing and Application of Kaolins, Bentonites, Palygorskite–Sepiolite and Common Clays: Developments in Clay Science, Volume 2, Elsevier, Netherlands; pp. 179.

Murray, H.H., 1980. Diagnostic tests for evaluation of kaolin physical properties. Acta Mineralogica 24, 1-24.

Murray, H.H., 1999c. Applied clay mineralogy today and tomorrow. Clay Minerals 34 (1), 39-49.

Murray, H.H., 2007. Applied clay mineralogy. Development in Clay Science 2. Elsevier, B.V.

Murray, H.H., Alves, C.A., Bastos, C.H., 2007. Mining, processing and applications of the Capim Basin kaolin, Brazil. Clay Minerals 42 (2), 145-151.

Murray, H.H., Keller, W.D., 1993. Kaolin. in: Murray, H.H., Bundy, W., Haevery, C. (Eds.), Kaolin genesis and utilization. : Special Publication, 1. Clay Minerals Society, Boulder, Co, USA, pp. 1-24.

Ngun, B.K., Mohamad, H., Sulaiman, S.K., Okada, K., Ahmad, Z.A., 2011. Some ceramic properties of clays from Central Cambodia. Applied Clay Science 53, 33–41. https://doi.org/10.1016/j.clay.2011.04.017

Njoya D., Hajjaji, M., Baçaoui, A., Njopwouo, D., 2010. Microstructural characterization and influence of manufacturing parameters on technological properties of vitreous ceramic materials. Materials Characterization 61, 289–295.

Nkoma, J., Ekosse, G., 1999. X-ray diffraction study of clays used for making bricks at Lobatse: montmorillonite, Illite and kaolinite. Botswana Journal of Earth Sciences 4, 28-33.

Oti, J. E., Kinuthia, J. M., and Bai, J., 2009. Engineering properties of unfired clay masonry bricks. Engineering Geology, 107(3e4), 130-139.

Pardo, F., Jordan, M.M., Montero, M.A., 2018. Ceramic behaviour of clays in Central Chile. Appl. Clay Sci. 157, 158–164. https://doi.org/10.1016/j.clay.2018.02.044.

Peng, L., Qin, S., 2019. Sintering Behavior and Technological Properties of Low-Temperature Porcelain Tiles Prepared Using a Lithium Ore and Silic Crucible Waste. Minerals 9, 731; doi:10.3390/min9120731

Pohl, W., Horkel, A., 1980. Notes on the Geology and Mineral Resources of the Mtito Andei-Taita Area (Southrn Kenya). Mitt, osterreichhische Geologische Gesellschaft 73, 135-152.

Ranogajec J., Djuric M., Radeka, M., Jovanic, P., 2000. Influence of particle size and furnace atmosphere on the sintering of powder for tiles production. Ceramics-Silikáty 44, 71–77.

SANS 227:2007 and SANS 1 575. 2007. The South African National Standard for burnt clay paving units, ISBN 978-0-626-19745-2

Selley, R., 2000. Applied sedimentology. San Diego, Calif.: Academic Press, p.430.

Semiz, B., 2017. Characteristics of clay-rich raw materials for ceramic applications in Denizli region (Western Anatolia). Appl. Clay Sci. 137, 83–93.

Serra, M F, Acebedoa, M S Conconia, G Suareza, E F. Aglietti, Rendtorff M.N., 2014. Thermal evolution of the mechanical properties of calcareous earthenware. Ceramics International 40 1709–1716

Serra, M., Conconi, M., Suarez, G., Agietti, E. and Rendtorff, N., 2013. Firing transformations of an Argentinean calcareous commercial clay. Cerâmica, 59(350), pp.254-261.

Shemang, E.M., Suh, C.E., Coetzee, S.H., 2007. Crystal morphology and indicative microchemistry of kaolinite from kaolin occurrences in Alkaleri region, northeastern Nigeria. GeoActa 6, 15-26.

Souza G.P., Sanchez R. and de Holanda J.N.F., 2002. Characteristics and physical-mechanical properties of fired kaolinitic materials. Cerâmica, 48(306), 102-107.

Strazzera, B., Dondi, M., Marsigli, M., 1997. Composition and ceramic properties of Tertiary clays from Southern Sardinia (Italy). Applied Clay Science 12, 247–266.https://doi.org/10.1016/S0169-1317(97)00010-0.

Teixera, S.R., Souza, S.A., Moura, C.A., 2001. Mineralogical characterization of clays used in the structural ceramic industry in West of Sao Paulo State, Brazil. Cerâmica 47(304), 204–207.

Temga JP, J R Macheb, A B Madi, J P Nguetnkam, D Bitom, L., 2019. Ceramics applications of clay in Lake Chad Basin, Central Africa. Applied Clay Science 171;118–132 https://doi.org/10.1016/j.clay.2019.02.003

Tsolis-Katagas, P., Mavronichi, M., 1989. Kaolinization of the Kimolos Island Volcanics, Cyclades, Greece. Clay Minerals 24, 75-79.

Van Reenen D. D., Roering C, Smit C. A. and Barton J. M. Jr., 1990. The Granulite Facies Rocks of the Limpopo Belt, South Africa. In: Vielzeuf D. and Vidal P. (Editors).

Granulites and Crustal Evolution NATO-ASI Series C211, Luwer, Dordrecht. pp. 257-289.

Velde, B.,1995. Composition and mineralogy of clay minerals, in Velde, B., ed., Origin and mineralogy of clays: New York, Springer-Verlag, p. 8-42.

Viania, A., Cultrone, G., Sotiriadis, K., Ševčík, R., Šašek, P., 2018. The use of mineralogical indicators for the assessment of firing temperature in fired-clay bodies. Applied Clay Science 163, 108–118. https://doi.org/10.1016/j.clay.2018.07.020.

Vieira, C.M.F., Sanchez, R., Monteiro, S.N., 2008. Characteristics of clays and properties of building ceramics in the state of Rio de Janeiro, Brazil. Constr. Build. Mater. 22,781–787.

Walker, P. J., 1999. Bond characteristic of earth block masonry. Journal of Materials in Civil Engineering, 11(3), 249-256.

Winkler H. G. F., 1954. Importance of particle size distribution and mineral content of clays for the production of heavy clay products.

Yongue-Fouateu R, Ndimukong, F, Njoya A, Kunyukubundo, F, Paul KM., 2016.The Ndop plain clayey materials (Bamenda area – NW Cameroon):Mineralogical, geochemical, physical characteristics and properties of their fired products. Journal of Asian Ceramic Societies 4, 299–308

Yuan, J., Murray, H.H., 1993. Mineralogical and physical properties of the Maoming kaolin from Guangdong Province, South China. In: Murray, H.H., Bundy, W., Harvey,

C. (Eds.), Kaolin genesis and utilization.: Special Publications No. 1. Clay Minerals Society, Boulder, Co, USA, PP. 249-260.